CLIMATE-INDUCED TRENDS IN GLOBAL RIVERINE WATER DISCHARGE AND SUSPENDED SEDIMENT DYNAMICS IN THE 21ST CENTURY

by

NISHANI POORNA MORAGODA

SAGY COHEN, COMMITTEE CHAIR
SARAH PRASKIEVICZ
HAMID MORADKHANI

A THESIS

Submitted in partial fulfillment of the requirements
for the degree of Master of Science
in the Department of Geography
in the Graduate School of
The University of Alabama

TUSCALOOSA, ALABAMA

2019

ABSTRACT

Anthropogenic climate change, particularly through increased greenhouse gas (GHG) emissions, is projected to considerably impact 21st century precipitation distribution, altering fluvial processes such as sediment dynamics and riverine water discharge, worldwide. Changes in the magnitude of fluvial water and sediment fluxes can have profound impacts on the functioning and connectivity of earth's natural systems. This study is focused on isolating the impacts of GHG-induced future climate change on riverine water discharge and suspended sediment fluxes in the 21st century at a global scale. A global-scale hydro-geomorphic model (WBMsed) was forced with precipitation and temperature projections generated from five General Circulation Models (GCMs), each driven by four Representative Concentration Pathways (RCPs).

The results, based on an ensemble of model outputs, revealed that global river discharge and sediment dynamics are considerably impacted by anthropogenic climate change in the 21st century. Despite substantial regional heterogeneity, a global net increase is projected for both river discharge and sediment flux in the 21st century under all RCP scenarios. Increases are larger and more variable with increasing levels of GHG concentrations in the atmosphere. At the end of this century, climate change under RCP 2.6 is projected to cause approximately 1% increase in global river discharge and 5% increase in global suspended sediment flux. Under RCP 4.5 emission scenario, climate change will lead to a 5.6% increase in river discharge and 7% increase in sediment flux at a global scale. Approximately 5% and 9% increases are projected

under RCP 6.0 in global river discharge and sediment flux respectively. Climate changes projected under RCP 8.5 will lead to the largest increases in river discharge and sediment flux (7.3% and 14.7% respectively) at the end of the 21st century.

With increased warming, more extreme changes (increasing or decreasing) can be expected in both discharge and sediment flux. Also, the number of rivers with statistically significant trends in either direction increases with warming. In addition to magnitudes, inter-annual variability in both global river discharge and sediment fluxes also increase with increasing RCPs. Changes in sediment flux closely follow the patterns predicted for discharge, and are mostly driven by climate warming induced spatial and temporal variation in precipitation. However, the relationship between discharge and sediment flux was found to be non-linear both in space and time, demonstrating the utility of explicit modeling of both hydrology and geomorphology.

DEDICATION

To my loving family…

LIST OF ABBREVIATIONS AND SYMBOLS

$Q_{s_{[i]}}$	Daily sediment flux
$\bar{Q}_s$	Long-term average suspended sediment load
$\bar{V}_l$	Average of the variable in the last decade of the 21st century
$\bar{V}_p$	Average of the variable in the last decade of the 21st century
$C_{(a)}$	Sediment rating parameter
E_h	human-influenced soil erosion factor
$Q_{[i]}$	Daily water discharge
$\bar{Q}$	Long-term average discharge
T_E	Trapping of sediment due to reservoirs
V_{pc}	Percentage change between the last decade and the present decade in any of the above variables
$\psi_{[i]}$	Exponential distribution as a function of $\bar{Q}$
*	Multiplied by
$°C$	Degrees Celcius
<	Less than
=	Equal to
>	Greater than
A	Basin upstream contributing area
arc-min	Minute of arc

ArcGIS	Geographical Information System software
BMA	Bayesian Model Averaging
CMIP5	Coupled Model Inter-comparisons Project Five
CO_2	Carbon dioxide
CV	Coefficient of variation
GCM	General Circulation Models
GHG	Greenhouse Gas
H1	Hypothesis 1
H2	Hypothesis 2
I	Glacial erosion processes
IPCC	Intergovernmental Panel on Climate Change
ISI-MIP	Inter-Sectoral Impact Model Intercomparison Project
kg/s	Kilograms per second
km	Kilometers
km^2	Square kilometers
L	Lithology
M&S92+	Milliman and Syvitski (1992) database
m^3/s	Cubic meters per second
NetCDF	Network Common Data Form
NWIS	National Water Information Systems
º N	Degrees North
º S	Degrees South
ppm	Parts per million

R	Difference in upstream relief
R^2	Coefficient of determination
RCP	Representative Concentration Pathways
SD	Standard deviation
T	Basin-averaged temperature of the upstream contributing area
USGS	United States Geological Survey
w	Coefficient of proportionality
W/m^2	Watt per square meter

ACKNOWLEDGMENTS

I wish to express my sincere gratitude to my adviser and mentor, Dr. Sagy Cohen, for his dear advice, guidance, encouragement and provision of a contented atmosphere for me to carry out my research, successfully.

I would also like to extend my appreciation to my committee members Drs. Sarah Praskievicz and Hamid Moradkhani for providing me with valuable input to further improve this work.

Most of all I would like to thank my husband Dinuke for motivating me to pursue greater heights, helping me to find better solutions for difficult problems, and for being the shoulder to fall on during challenging times. I also thank my family in Sri Lanka for their continued encouragement and support.

I am thankful to my fellow lab mates, especially Austin Raney for helping me to overcome technical and programming challenges during the data analyses phase of this research.

I regret not being able to mention the names of each and every one individually, but your contribution is highly cherished and prized in the successful completion of this research.

CONTENTS

LIST OF TABLES

LIST OF FIGURES

LIST OF EQUATIONS

CHAPTER 1

INTRODUCTION

Human influence on the climate through anthropogenic greenhouse gas (GHG) emissions are highest in the history and according to the Intergovernmental Panel on Climate Change (IPCC), the resulted warming of the climate system has led to unprecedented changes in global climate (IPCC, 2014). Climate warming is projected to continue in the future with continued emission of GHGs leading to long-term changes in all components of the climate system (Arnell, 2003; Milly et al., 2005), with high possibility of irreversible and severe impacts on the environment (IPCC, 2014). Effects on the hydrological cycle due to climate change are observed in many regions, altering the quantity and quality of available water resources (Bates et al., 2008). This has placed increased attention on the future of global rivers and how impacts of climate changes are manifested through the behavior of fluvial systems (Bates et al., 2008; Syvitski et al., 2003; Walling, 2009). A comprehensive understanding of the response of fluvial systems to future changes in climate warrants detailed analysis of future riverine water discharge and sediment fluxes (Shrestha et al., 2016).

Sediment transport by rivers plays an essential role in the functioning and connectivity of the earth's natural systems, by directly influencing ecohydrological, biogeochemical and geomorphological processes (Vörösmarty et al., 2003; Walling and Fang, 2003). The magnitude of sediments transported by rivers is key to studying carbon and nutrient cycles, contaminant pathways, and biodiversity and habitat conditions in riverine, coastal and marine ecosystems

(Mukundan et al., 2013; Syvitski and Milliman, 2007; Walling, 2009). Sediments are also responsible for structuring landscape features such as deltas and controlling channel geometry and morphology (Pelletier, 2012; Vercruysse et al., 2017). The transport of sediment from rivers to the oceans is particularly important in deltaic coasts, as the survival of deltas depends on the continued supply of sediment (Darby et al., 2015). Sediment loads transported by the global rivers also serve as an important sensitive indicator of the changes in the Earth's processes (Fryirs, 2013; Walling, 2009). In addition to the key role in natural planetary functions, sediment dynamics has important engineering and socio-economic implications on dam sustainability, flood hazard and associated damages to infrastructure, and water quality (Vercruysse et al., 2017). Thus, changes in sediment transport by world's rivers can have impacts at global as well as regional and local scales. Although there is extensive literature with regard to estimation of sediment fluxes (e.g. Pelletier, 2012; Syvitski and Milliman, 2007; Syvitski et al., 2003; Walling and Fang, 2003), simulating global riverine sediment fluxes still remain challenging owing to the multiscale nature (Cohen et al., 2014; Pelletier, 2012; Vercruysse et al., 2017) and the non-linear relationship (Coulthard et al., 2012; Fryirs, 2013) of the processes involved.

A major factor affecting changes in sediment transport and river discharge is climate (Aerts et al., 2006; Haddeland et al., 2014; Syvitski, 2003a; Syvitski, 2003b). Projected future changes in climate, particularly rises in temperature driven by increased GHG emissions, are projected to considerably alter 21st century precipitation intensity and distribution (IPCC, 2014; Lu et al., 2013; Oki and Kanae, 2006; Pendergrass et al., 2017). These changes in temperature and precipitation are the major climatic factors that alter fluvial processes including river discharge and sediment fluxes worldwide (Lu et al, 2013; Pelletier, 2012; Syvitski, 2003a; Zhu et al., 2008). Research has shown that relatively moderate shifts in average climate conditions (i.e.

changes of 1-2^{0}C, 10-20% precipitation) have considerable impacts on the behavior of rivers, especially with regard to flood response and thus sediment yield (Knox, 1993; see Syvitski, 2003b). Not only average climate conditions but also, projected increases in extreme events due to climate change can have profound and complex impacts on hydrological responses of a catchment (Fryirs, 2013; Julien, 2010). Future climate change driven impacts on river flows have implications on available water resources, and possible drought and flood conditions (Arnell, 2003; Nakaegawa et al., 2013; Schewe et al., 2014). Detailed estimates of future fluvial sediment fluxes and river discharges is, therefore, needed in order to predict and prepare to climate change impacts on natural planetary functions, and human-related activities and wellbeing.

The role that basin-wide temperature plays on sediment discharge is important in terms of the rate of chemical breakdown of rocks and soil formation (Yang et al., 2015). Syvitsky et al. (2003) found an increase in both soil erosion rates and sediment yield with increasing temperature. Temperature also controls the pathway of precipitation, and rate and timing of snow melt, which in turn affect river flow and sediment transport. Precipitation directly influences the discharge of rivers (Arnell, 2003; Rodríguez-Blanco et al., 2016; Syvitsky et al., 2005) and is a major driver of soil erosion that affects sediment loads (Mukundan et al., 2013; Pelletier, 2012; Yang et al., 2015). This largely depends on the intensity, duration and other rainfall characteristics (Zhu et al., 2008). In addition, the sediment yield responses in different regions for a given climatic event may also vary depending on the drainage area, spatial variability in relief, geology and other hydrological processes (Syvitski, 2003b; Vercruysse et al., 2017). The different responses of catchment scale sediment dynamics to climate change led Walling and Webb (1983) conclude that, "Current evidence concerning the relationship between climate and sediment yield emphasizes that no simple relationship exists."

Human interferences on hydrological systems such as damming, soil conservation measures, irrigation networks etc. also have substantial influences on discharge and sediment loads carried by rivers (Walling, 2009; Wang et al., 2011, Syvitski et al., 2005). The increasing impacts of both human activities and climate change on river systems necessitates the need to identify and quantify the impacts from individual drivers on fluvial water and sediment discharge (Yang et al., 2015). Therefore, it is import to isolate the effects of changing climate as one of the primary drivers of changes in fluvial systems, and this allows more informed decision making with regard to human activities affecting hydrological systems. However, in most cases, it is difficult to disentangle the signal of climate from other human impacts (Lu et al., 2013; Walling, 2009). Numerical models to this end are considered a useful tool to study these changes. They not only offer insights into future and past trends associated with various drivers of change (Cohen et al., 2014), but also help fill the gaps in sediment dynamic measurements (Coulthard et al., 2012). The complex responses of river discharge and sediment fluxes to spatial and temporal dynamics of future climate change warrants sophisticated distributed numerical models (Cohen et al., 2014). A spatially and temporally explicit global-scale riverine sediment flux model, WBMsed (Cohen et al., 2013, 2014) was used in this study to simulate future suspended sediment load and river discharge dynamics in response to future climate change.

1.1 Climate Scenarios

Given the uncertainties in factors such as population growth, economic development, technological advancement, social and environmental conditions, that can contribute to future climate change and its impacts, ‘emission scenarios’ have long been used, to provide alternative plausible descriptions of future climate trajectories. Over time, these scenarios have evolved

from simple conventional approaches based on annual percentage rises in global average GHG concentrations, to more advanced approaches involving emissions of numerous gases and particles along with socioeconomic and technology assumptions that can influence Earth's climate (Bjørnæs, 2013; Van Vuuren et al., 2011).

The latest generation of scenarios, known as Representative Concentration Pathways (RCPs), were introduced by the IPCC as the base of the findings of its fifth assessment report (IPCC, 2014). There are four RCPs that provide quantitative descriptions of concentrations of the climate change pollutants in the atmosphere over time, as well as their radiative forcing (measure of the additional energy taken up by the earth system due to the enhanced greenhouse effect) (Bjørnæs, 2013). The four RCP scenarios are:

RCP 8.5 – High emissions: No policy changes to reduce emissions. Characterized by increasing GHG emissions that lead to high GHG concentrations over time. This trajectory reaches a radiative forcing of 8.5 W/m^2 (~ 1370 ppm atmospheric CO_2 equivalent) by 2100, and will continue to rise.

RCP 6.0 – Intermediate emissions: Stabilizes the radiative forcing at 6.0 W/m^2 (~ 850 ppm atmospheric CO_2 equivalent) shortly after 2100, by the application of a range of technologies and strategies for reducing GHG emissions.

RCP 4.5 – Intermediate emissions: Radiative forcing of 4.5 W/m^2 (~ 650 ppm atmospheric CO_2 equivalent) that stabilizes shortly after 2100. Relatively ambitious emission reductions.

RCP 2.6 – Low emissions: Radiative forcing reaches a peak of 3 W/m^2 (~ 490 ppm atmospheric CO_2 equivalent) and then declines to 2.6 W/m^2 by 2100. Low radiative forcing levels which can only be achieved with ambitious GHG emission reductions over time.

1.2 General Circulation Models

Future climatic changes over this century and beyond can be projected under these scenarios by using future-predicting climate models. These highly sophisticated climate models are the primary tools currently available for investigating the response of climate systems to various forcings (Flato et al., 2013). Global-scale studies exploring the impacts of these changes in climate on surface hydrology are often based on the results generated by General Circulation Models (GCMs) (Sperna Weiland et al., 2012). However, individual GCMs may produce varying and sometimes contradictory results, especially for precipitation (Covey et al., 2003; Krakauer and Fekete, 2014).

In this study, precipitation and temperature projections produced by five GCMs which participated in the Inter-Sectoral Impact Model Intercomparison Project (ISI-MIP) are used. ISI-MIP is an initiative aiming at projecting the impacts of various levels of global warming based on the RCP scenarios, using an ensemble of GCMs representing climate impacts in different sectors (such as water, biomes, agriculture, health, infrastructure) (ISIMIP, 2019; Warszawski et al., 2014). The ISI-MIP, is a subset of five GCMs from the Coupled Model Inter-comparisons Project Five (CMIP5), and is widely used in global climate impact studies (Haddeland et al., 2014; Hattermann et al., 2018; McSweeney and Jones, 2016; Schewe et al., 2014). The five GCMs of the ISI-MIP used in this study are: GFDL-ESM2M, HadGEM2-ES, IPSL-CM5A-LR, MIROC-ESM-CHEM and NorESM1-M. The ISI-MIP provides daily resolution climate data for these GCMs that have been statistically downscaled to a 0.5º X 0.5º latitude-longitude grid using bilinear interpolation in space, and then bias-corrected by observational data on the grid using a trend preserving method. The ISIMIP statistical downscaling and bias adjustment method is comprehensively described in Hempel et al. (2013), Frieler et al. (2017), and Lange (2019). A

number of studies that used GCMs in predicting the future response of rivers to climate change highlighted that the choice of GCMs highly influenced the calculated changes, and therefore a multi-model ensemble of GCMs provides the most reliable impressions on the spread of possible changes (IPCC, 2014; Sperna Weiland et al., 2012). Following the studies including Hagemann et al. (2013), Milly et al. (2005), Nohara et al. (2006) and Nijssen et al. (2001) we also used the multi-model ensemble method when assessing the possible impacts.

1.3 Research gaps

A number of studies have been carried out to explore the recent trends in discharge and suspended sediment loads in global rivers at a range of scales (e.g. Cohen et al., 2014; Syvitski, 2002; Syvitsky et al., 2003; Walling and Fang, 2003; Wang et al., 2011). Attempts to investigate basin scale sediment load dynamics provide evidence of marked changes in the sediment loads and water discharge and contrasting trends in recent years (Dai et al., 2009; López and Torregroza, 2017; Walling, 2009). In many instances, these changes are attributed to the interaction between climate change and human impact (Syvitsky, 2003b; Walling and Fang, 2003; Wang et al., 2011).

Studies have also been conducted to estimate the potential effects of future climate change on river discharge and sediment flux. Although there is a wealth of literature related to the effects of GHG-induced global warming on future discharge of rivers at a global scale (Aerts et al., 2006; Arnell, 2003; Döll and Zhang, 2010; Milly et al., 2005; Nakaegawa et al., 2013; Nijssen et al., 2001; Nohara et al., 2006; Sperna Weiland et al., 2012; van Vliet et al., 2013), assessments of sediment flux in response to climate change are mostly in river catchment scale (Coulthard et al., 2012; Darby et al., 2015; Lu et al., 2013; Rodríguez-Blanco et al., 2016;

Shrestha et al., 2016; Ward et al., 2009; Yang et al., 2015, Zhu et al., 2008). At a global scale, attempts have been made to quantify the effects of changes in climate and land use/human activities together on sediment delivery (Syvitski and Milliman, 2007; Syvitski et al., 2003) and water discharge (Dai et al., 2009; Haddeland et al., 2014; Zhu et al., 2012) by rivers to the oceans. Global scale studies on the influence of climate change on river sediment flux are limited (e.g. Pelletier, 2012; Syvitski, 2003a).

Most of the research related to sediment flux estimates are retrospective assessments or attempts to estimate the present-day sediment fluxes, at a global-scale or individual river basin level (Morehead et al., 2003). Investigations of future climate change impacts on riverine fluxes are either focused on individual river systems or consider combined effects of both climate change and human activities on sediment delivery. Also, the studies that assessed the impact of future climate change on rivers have used climate change scenarios that were introduced prior to the IPCC's most recent report (Arnell, 2003; Milly et al., 2005; Nakaegawa et al., 2013; Nohara et al., 2006; Sperna Weiland et al., 2012; van Vliet et al., 2013).

This project is focused on isolating the impacts of future climate change from that of land use and anthropogenic activities on riverine water discharge and suspended sediment fluxes at a global scale. This is aimed at providing the first quantitative assessment of potential global fluvial response in the 21st century to all of the most recent future climate change trajectories introduced by the IPCC. This study is the first of its kind that provides a comprehensive and spatially explicit analysis of river discharge and suspended sediment flux responses to future GHG-induced climate change pathways at a global scale.

1.4 Goal and Hypotheses

The overarching goal of this study is to analyze future global suspended sediment and riverine water discharge dynamics in response to projected climate change in the 21st century. Changes in earth's climate system were incorporated by forcing a numerical model (WBMsed) with precipitation and temperature projections generated from five GCMs each driven by four RCPs. The following hypotheses were investigated:

H1: Increased GHG concentrations, represented by the four RCP scenarios, will lead to increases in the magnitude and variability in water discharge and fluvial sediment fluxes, at a global scale.

While changes in the GHG-induced global precipitation distribution are expected to vary considerably in different parts of the world (IPCC, 2014), from a global perspective, increases in GHG concentration trajectories (and associated global warming) are expected to lead to a cumulative net-increase in both sediment and water discharge. In addition, the variability in future precipitation is projected to increase over a majority of the global land area, in response to warming represented by RCP scenarios (Bates et al., 2008; Pendergrass et al., 2017). Therefore, the temporal variability in global riverine water discharge and suspended sediment fluxes is also expected to increase with increasing GHG concentration trajectories.

H2: Climate-induced temporal variability in suspended sediment fluxes and water discharge into global oceans will be larger in tropical and higher latitudes than mid latitudes for a given RCP scenario.

The magnitude of sediments transported to the global oceans from fluvial systems over time, plays an important role as a measure of sustainability of the coastal zone, in the face of

increased coastal flood susceptibility and sea level rise (Darby et al., 2015). It is expected that there will be significant basin-to-basin and continent-to-continent variability in river discharge and suspended sediment delivery into the global ocean, given the spatial and temporal variability in future climatic conditions (Syvitski, 2003b). The basis for this hypothesis is the projected increase in future precipitation variability in the Inter Tropical Convergent Zone and in the high latitudes of both hemispheres, by climate models (Pendergrass et al., 2017). Given that variability in precipitation has major effects on water discharge and sediment dynamics (Cohen et al., 2014; Dai et al., 2009), it is reasonable to hypothesize that latitudinal variability in these two variables will be governed by the climate-induced temporal variability in precipitation.

1.5 Objectives

- Investigate temporal trends and variability in future riverine fluxes in large global rivers in response to increasing levels of GHG-induced climate change

- Analyze temporal and spatial variability in future global river discharge and sediment delivery into global oceans from large river outlets, between continents, major river basins and latitudinal regions.

- Identify the regions that will experience significant changes in river discharge and suspended sediment loads in the 21st century in response to climate change.

CHAPTER 2

METHODOLOGY

2.1 Numerical simulations

2.1.1 Model description

Global riverine water discharge and suspended sediment fluxes were simulated using the spatially and temporally explicit global riverine sediment flux model WBMsed v2.0 (Cohen et al., 2014). The WBMsed model incorporates a variety of parameters related to climate (precipitation, temperature, solar radiation), surface (lithology, topography, relief, riverine) and anthropogenic effects (dams, irrigation, land use). It is an extension of the WBMplus global hydrology model (Wisser et al., 2010; see Cohen et al., 2013), and is a spatially and temporally explicit implementation of the BQART (Syvitski and Milliman, 2007) and Psi (Morehead et al., 2003) basin outlet sediment load equations. The WBMsed model considers each pixel as an outlet of its upstream contributing area and its own area, for the purpose of continuously simulating these models in space (Cohen et al., 2013). The model governing sediment flux, BQART, simulates long-term (>30 years) average suspended sediment loads ($\bar{Q}_s$) for a basin outlet as follows,

$$\bar{Q}_s = wB\bar{Q}^{0.31}A^{0.5}RT \quad \text{for } T \geq 2°C \tag{1a}$$

$$\bar{Q}_s = 2wB\bar{Q}^{0.31}A^{0.5}R \quad \text{for } T < 2°C \tag{1b}$$

where w is the coefficient of proportionality in units of kg/s which equals to 0.02, $\bar{Q}$ is the long-term average discharge (m^3/s), A is the basin upstream contributing area (km^2), R is the difference in upstream relief (km), and T is the basin-averaged temperature of the upstream contributing area ($°C$). The term B accounts for glacial erosion processes (I), lithology (L), trapping of sediment due to reservoirs (T_E) and a human-influenced soil erosion factor (E_h) (Syvitski and Milliman, 2007):

$$B = IL(1 - T_E)E_h \tag{2}$$

The Psi equation (Morehead et al., 2003) is used in WBMsed to calculate daily sediment load and is capable of capturing the intra- and inter-annual variability observed in natural river systems (Morehead et al., 2003; see Cohen et al., 2014):

$$\left(\frac{Q_{s[i]}}{\bar{Q}_s}\right) = \psi_{[i]} \left(\frac{Q_{[i]}}{\bar{Q}}\right)^{C_{(a)}} \tag{3}$$

where $Q_{s_{[i]}}$ is daily sediment flux (kg/s), $Q_{[i]}$ is daily water discharge (m3/s), $\psi_{[i]}$ is an exponential distribution as a function of $\bar{Q}$ where ψ is large for small rivers and ψ is small for large rivers, $C_{(a)}$ is a sediment rating parameter, that varies on a spatial and temporal scale as a function of R and $\bar{T}$ (Morehead et al., 2003; see Cohen et al., 2014). This gives the model the capability to reflect the temporal variability in Q-Qs relationship between different rivers (Cohen et al., 2014). Syvitski (2003a) states that climate influences on the sediment load variability in rivers are mainly explained by $Q_{[i]}/\bar{Q}$ ratio (as proxy to flood wave dynamics) and $C_{(a)}$ rating coefficient (as proxy to sediment transport efficiency). The water discharge module of the WBMsed model takes into account precipitation, evapotranspiration, infiltration, soil moisture, irrigation, reservoirs, diversions, and floodplain retention, and is based on the WBMplus model

(Wisser et al., 2010; see Cohen et al., 2013). The WBMsed model is proven to be successful in predicting suspended sediment loads in global rivers and studying different mechanisms and drivers associated with these processes (e.g. Cohen et al., 2013, 2014; Syvitski et al., 2014; Taylor et al., 2015).

2.1.2 Simulation settings

In this global-scale analysis, the model was used to simulate long-term suspended sediment loads and river discharges through the 21st century under RCP 2.6, RCP 4.5, RCP 6.0 and RCP 8.5 scenarios. In order to investigate the response of future climate changes, daily precipitation and temperature projections generated by the five GCMs (GFDL-ESM2M, HadGEM2-ES, IPSL-CM5A-LR, MIROCESM- CHEM and NorESM1-M) were used as climate inputs to the WBMsed model. Both the hindcast (1950 – 2005) and future (2006 – 2099) climate data obtained from the GCMs were used to force the WBMsed model. The absolute values of the GCM projections were used instead of a change factor method (as used by Arnell (2003), Nijssen et al. (2001), Vörösmarty et al. (2000)), as this gives more reliable estimates for changes in climate variability and extremes (Sperna Weiland et al., 2012). For this study, climate projections generated by GCMs which were downscaled to 0.5º * 0.5º resolution by the ISI-MIP were used, given the global scale nature of the simulations and the associated coarse resolution. Most if not all the comparable studies done at a global scale have used this or more coarser resolution climate data (Aerts et al., 2006; Arnell, 2003; Haddeland et al., 2011, 2014; Hirabayashi et al., 2008; Nakaegawa et al., 2013; Nijssen et al., 2001; Nohara et al., 2006; Sperna Weiland et al., 2012; van Vliet et al., 2013; Vörösmarty et al., 2000).

In order to isolate the signal of climate on the changes in discharge and sediment flux, the model simulations were conducted in the WBMsed 'pristine' mode which exclude all anthropogenic input parameters, in its sediment and hydrological modules. In the sediment module, in pristine mode, the T_E and E_h parameters are set to a value of 1 (neutral). In the hydrological simulation, all anthropogenic drivers are excluded including irrigation, ground and surface water uptake, agriculture-affected evapotranspiration, dam operation, and water retention in man-made reservoirs.

Separate simulations were conducted in the WBMsed model for climate data generated by each GCM for each RCP scenario leading up to 20 simulations with the combination of 5 GCMs and 4 RCP scenarios. Each simulation was conducted for both historical and future periods to output monthly and annually averaged (the model simulations are at daily time steps) river discharge and suspended sediment flux for the entire globe at a 6 arc-min (~11 km) spatial resolution. The simulations were performed on the University of Alabama High Performance Computing Cluster.

2.1.3 Creating the multi-model ensemble

The model outputs (in NetCDF file format) were used to create the multi-model ensembles for discharge, suspended sediment flux, temperature and precipitation separately, using a Python script. The WBMsed outputs generated in response to each of the five GCMs were averaged for each year separately to get the ensemble and this was done for each RCP. A non-weighted mean from each GCM based run was created, as weights derived from hindcast performances may not hold for the future period and therefore can be misleading (Sperna Weiland et al., 2012). This created NetCDF files that contain the ensemble of all GCM based

runs for each year from 1950 to 2099, for all the four RCPs, and for discharge, sediment flux, temperature and precipitation. They were then used for subsequent analyses.

2.1.4 Model validation

The WBMsed model has already been validated for the long-term average of predicted fluxes (using observed climate data inputs) against measured fluxes across the United States and global sites (Cohen et al., 2013 and 2014). In order to validate the model performance for GCM based runs against observed fluxes, the long-term average of the multi-model ensembles throughout the hindcast period (1950-2005) for both discharge and suspended sediment flux were used. The observed discharge and suspended sediment fluxes were obtained from the USGS National Water Information Systems (NWIS) website (U.S. Geological Survey, 2018), and Milliman and Syvitski (1992) database (M&S92+). The validation against USGS sites was done for the long-term average of daily discharge and sediment flux data for 36 USGS sites that has drainage areas > 10,000 km^2, average water discharge > 30 m^3/s, and with at least 20 years of daily data. The long-term average sediment flux and discharge data obtained for 133 sites were used for the validation against M&S92+ database. For both observational datasets, the time-averaged values do not represent the entire period of the model output (1950-2005).

2.2 Trend and variability analyses

2.2.1 Changes in future climate, river discharge and suspended sediment fluxes relative to the present

The ensemble model outputs were visualized and analyzed using ArcGIS 10.6 software and Python and R scripting. Changes in discharge, sediment flux, temperature and precipitation in the last decade (2090-2099) relative to the present decade (2010-2019) of the 21st century

were calculated based on the multi-model ensemble projections for each RCP scenario according to the following equation:

$$V_{pc} = \frac{(\bar{V}_l - \bar{V}_p)}{\bar{V}_p} \quad (4)$$

where V_{pc} is the percentage change between the last decade and the present decade in any of the above variables, $\bar{V}_l$ is the average of the variable in the last decade (2090-2099) of the 21st century and $\bar{V}_p$ refers to the average of the variable in the present decade (2010-2019) of the 21st century for a given RCP scenario (Sperna Weiland et al., 2012). Maps that show the global scale changes in discharge, sediment flux, temperature and precipitation in the last decade relative to the present decade of the 21st century were generated for each RCP.

In order to visually represent analyses results for discharge and suspended sediment flux in global rivers, a polyline shapefile of global rivers was used. This was done because the model resolution is too fine to clearly see river cells at a global-extent map. Upscaling the output raster resolution will greatly distort the values within the river cells, while GIS line features can be re-sized without modifying their values. Due to the limitations of the model predictive capabilities for small rivers (Cohen et al., 2014), grid cells with a contributing area < 10,000 km^2 and average water discharge < 30 m^3/s a were first masked using a raster layer. Then discharge and sediment flux data in unmasked pixels were extracted for river segments of the global rivers layer using "Zonal Statistics as Table" tool in ArcMap.

The change in future discharge and sediment delivery to global oceans from major rivers was also calculated. The pixel values in major river outlets were extracted for each RCP scenario for river outlets listed in Table 2. Furthermore, the average discharge and sediment delivery from all the river outlets in a given continent were calculated for the present decade and the last

decade of the 21st century separately, which was then used to calculate the percentage change in future discharge and sediment delivery to the oceans from each continent for each RCP.

2.2.2 Analysis of significant trends

Temporal trend analysis to identify significant trends in annual global sediment flux and water discharges was carried out for each RCP scenario to achieve objective 1 and to test the first hypothesis (H1). This was carried out for each grid-cell using the non-parametric Mann-Kendall trend test (Mann 1945, Kendall 1975) to statistically assess if there is any significant increasing or decreasing trends over time. First, separate layer stacks were created using annual ensemble NetCDF files for the period between 2006 – 2099 for discharge and sediment flux in each RCP scenario. Then the time series of discharge and sediment flux in each pixel throughout the future period were extracted separately. The Mann-Kendall trend test was performed for the time series in each pixel to output two separate raster layers with the p-values and Kendall's tau values for each pixel. The p-value raster was then used to identify pixels with significant trends at 95% confidence level and the direction of the change was identified using Kendall's tau raster. The pixels with significant trends in either direction were extracted to the global rivers layer after performing the masking procedure. Maps showing significant trends in discharge and sediment flux in global rivers and river outlets were created for each RCP. In order to assess the significant changes in discharge and sediment flux in the last decade relative to the present decade for rivers listed in Table 2, student t-test was used at 95% confidence level (Rodríguez-Blanco et al., 2016).

2.2.3 Variability analysis

In order to examine the changes in temporal variability in discharge and sediment flux with increasing RCP scenarios as hypothesized in H1, coefficient of variation (CV) was employed (Arnell, 2003). CV was selected rather than standard deviation (SD), as it gives the capability to compare between different RCPs and rivers of different sizes. The "Cell Statistics" tool in ArcMap was used to calculate the SD in discharge and suspended sediment load separately between the ensemble outputs throughout the future period. This resulted in a raster layer with SD values for each pixel. The same steps were followed to create raster layers of mean values for both discharge and sediment flux. Then a raster layer of CV (%) was created for both the variables and each RCP, using "Raster Calculator" tool in ArcMap as follows:

$$CV = \left(\frac{SD}{Mean}\right) \times 100 \quad (5)$$

In order to assess how the CV change between RCP scenarios, the ratio between a given RCP scenario and RCP 2.6 was calculated, by dividing the CV layer of a given RCP by that of RCP 2.6, for both discharge and sediment flux.

The temporal variability in discharge and sediment delivery to global oceans from river outlets between each latitudinal region was analyzed to test H2. A global river outlet layer of 555 outlets with a contributing area < 10,000 km^2 and average water discharge < 30 m^2/s was used. Mean discharge and sediment flux to global oceans from river outlets in each 1º latitudinal region was calculated for each year using the multi-model ensembles. This created annual time series of average discharge and sediment flux to oceans from each 1º latitudinal region for the time period between 2006 – 2099 for each RCP. Then the SD and mean of these time series were

calculated for each latitudinal region, from which CV was calculated using Eq. 5. Then the mean and the CV of each latitudinal region was plotted for each RCP scenario.

2.2.4 Relationship between discharge, sediment flux and projected future climate

Eight major rivers from around the world that represent different continents, latitudinal regions and various climatic conditions were selected to further investigate the future trends in discharge and sediment flux and how these trends are related to trends in basin averaged temperature and basin total precipitation. The eight river basins are: Yangtze river in China, Amazon river in South America, Mississippi river in North America, Nile river in Africa, Danube river in Europe, Lena river in Russia, Ganges and Brahmaputhra in Asia and Parana in South America. In order to evaluate the diverse responses of each GCM for a given RCP scenario, the time series of discharge and sediment flux of these river outlets were extracted for the ensemble as well as individual GCMs. In addition, a layer of global river basins was used to calculate basin-averaged temperature and basin-total precipitation for each river basin for each RCP.

CHAPTER 3

RESULTS

3.1 Model validation

Cohen et al. (2013, 2014) evaluated the WBMsed model predictions of long-term averaged suspended sediment flux and water discharge (using observed climate inputs) and found a correlation of $R^2 = 0.66$ to observed sediment flux and $R^2 = 0.70$ to water discharge data for 95 global sites. A stronger correlation was found to observed sediment flux for 11 USGS sites ($R^2 = 0.94$). In this study, the model's forecasting capability using GCM forcings was assessed based on the ensemble hindcast predictions.

The long-term averaged water discharge and suspended sediment loads evaluated against 133 global sites listed in M&S92+ database (Milliman and Syvitski, 1992), show that the ensemble of GCM based water discharge predictions correlate well ($R^2 = 0.85$) with observed data (Figure 1a), while sediment loads have a more moderate correlation of $R^2 = 0.66$ (Figure 1b). The validation of GCM based WBMsed hindcasts against 36 USGS sites across the continental United States also resulted in a similar correlation of $R^2 = 0.86$ for water discharge (Figure 1c) and $R^2 = 0.60$ for sediment loads (Figure 1d). The reason for the weaker correlation in the USGS sites compared to Cohen et al. (2013), is due to the use of 'pristine' simulations in this study. This has impacted the predictions in the US due to the considerable level of alteration compared to other global rivers. These results show that the ensemble of GCM based hindcast

WBMsed simulations can compare well to the model's 'standard' observational climate input dataset and can therefore be used with confidence for forecasting the future.

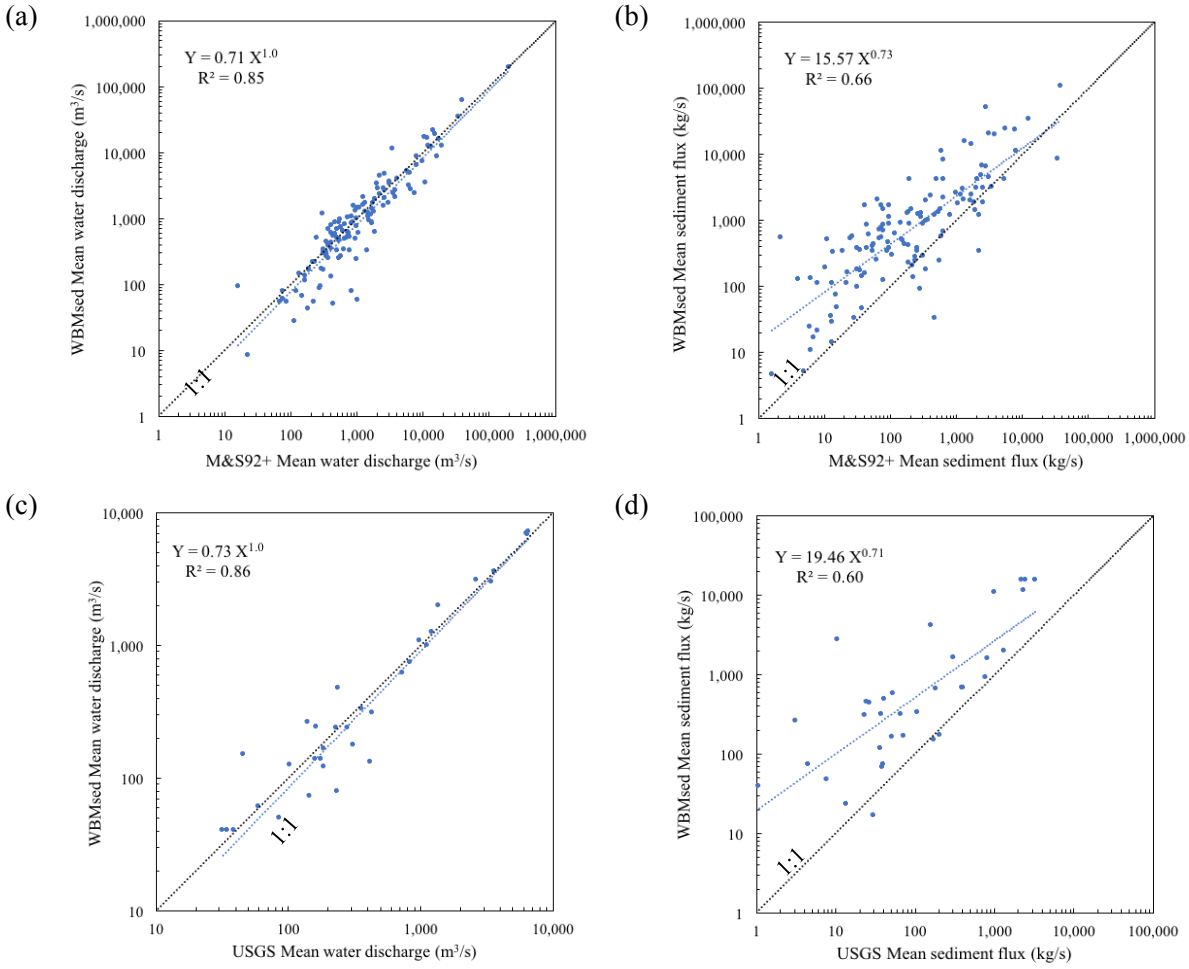

Figure 1: Comparison of long-term averaged GCM based hindcast sediment loads for 133 global sites against M&S92+ observed water discharge (1a) and sediment loads (1b), and for 36 US sites against USGS observed water discharge (1c) and sediment loads (1d).

This validation procedure only evaluates the predicted long-term river discharges and sediment fluxes. Although a validation of the time series of river discharges and sediment fluxes using other standard statistical methods could provide more insight into model's forecasting ability, it is not suitable for this study. The main reason is the fact that GCM based simulations

are conducted under the WBMsed pristine condition to exclude anthropogenic input parameters, and hence does not necessarily represent the real-world riverine fluxes. However, majority of the rivers in the US and outside are highly regulated by dam operations and other human water uses, and therefore have vastly controlled flows and sediment fluxes. In addition, freely available river discharge and suspended sediment flux records for the entire historical period is extremely rare outside the US and even in most US sites (Cohen et al., 2014). These reasons limit our ability to conduct a more comprehensive validation using the historical time series of simulated riverine fluxes based on GCM climate inputs.

3.2 Changes in global climate in the 21st century

Figures 2 and 3 show the changes in temperature and precipitation respectively, in the last decade of the 21st century relative to the present decade, using an ensemble of all five ISI-MIP climate model projections used as climate forcing data. Global temperature shows a clear increase at the end of the 21st century in all the RCPs and increases are larger with increasing warming scenarios (Figure 2). Decreases in temperature are observed only in RCP 2.6 (Figure 2a) in a few locations (e.g. east Africa, New Zealand). In all RCP scenarios, larger increases can be observed in the high latitudes of the Northern Hemisphere, in line with reported trends by the Fifth Assessment Report of the United Nations Intergovernmental Panel on Climate Change (IPCC, 2014).

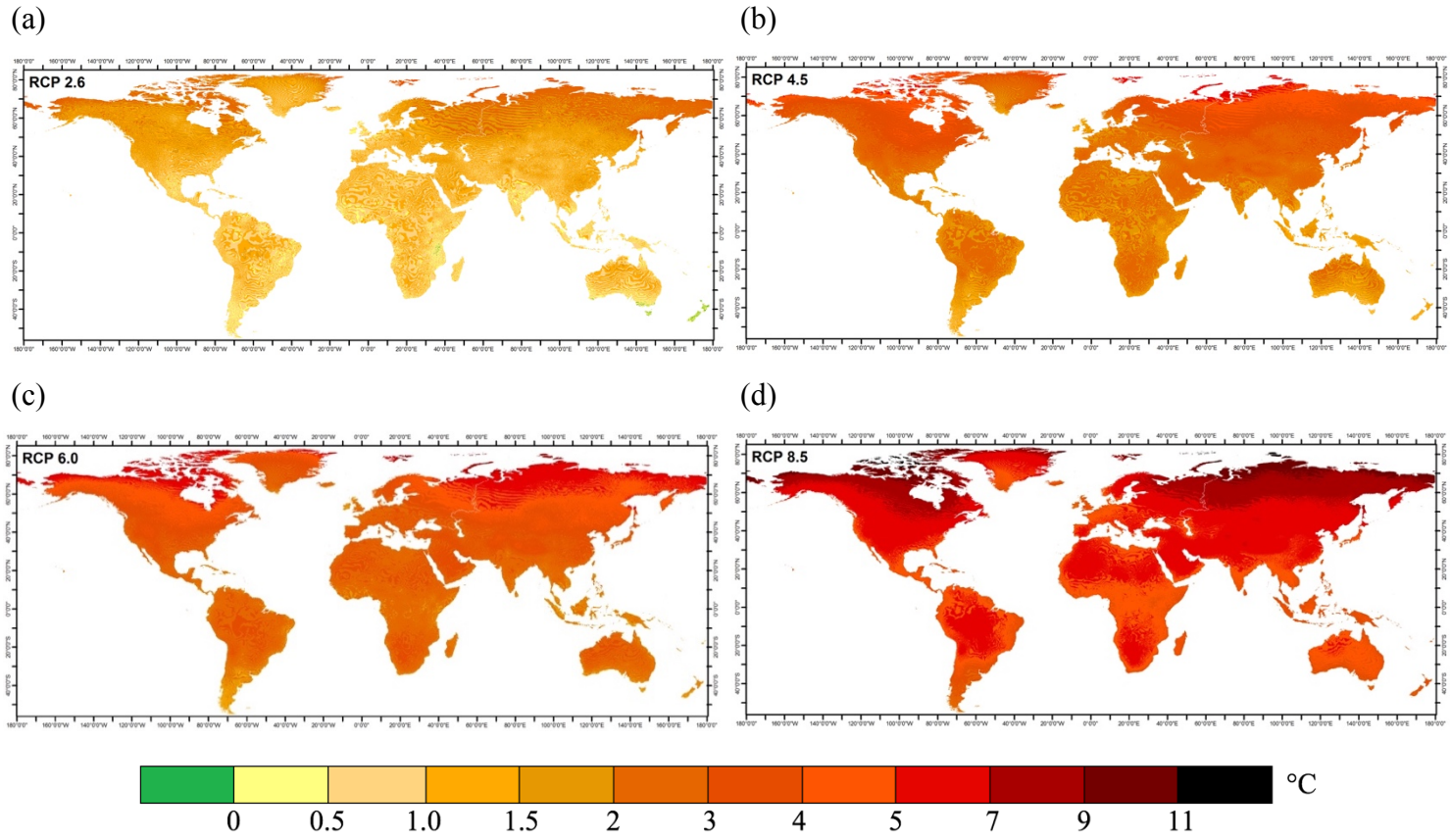

Figure 2: Change in global averaged land surface temperature in the last decade of the 21st century (2090-2099) relative to the first decade (2000-2010) under all RCP scenarios based on the multi model ensemble projections.

Changes in precipitation is not uniform (IPCC, 2014) and does not necessarily follow the changes in temperature (Figure 3). In different regions of the world, warming can lead to increases or decreases in precipitation. Larger increases in precipitation can be observed in high latitudes of the Northern Hemisphere, Sahel region in Africa and east Africa with increasing RCP scenarios, as previously suggested (Bates et al., 2008; Haarsma et al., 2005; Sylla et al., 2016). Precipitation also increases in majority of Asia including the middle eastern region, and parts of North America. Larger decreases in precipitation with increasing RCPs are observed in northern Africa, Mediterranean regions, southern and western Europe and some parts of Australia. In general, South America, southern regions of North America, Australia, southern regions of Africa and Western regions of Asia will experience decreases in precipitation. These maps prepared using the ensemble of ISI-MIP climate model projections are largely consistent with the predicted climate changes in the IPCC (2014) climate change synthesis report and other climate change studies (Pendergrass et al., 2017; Trenberth, 2011).

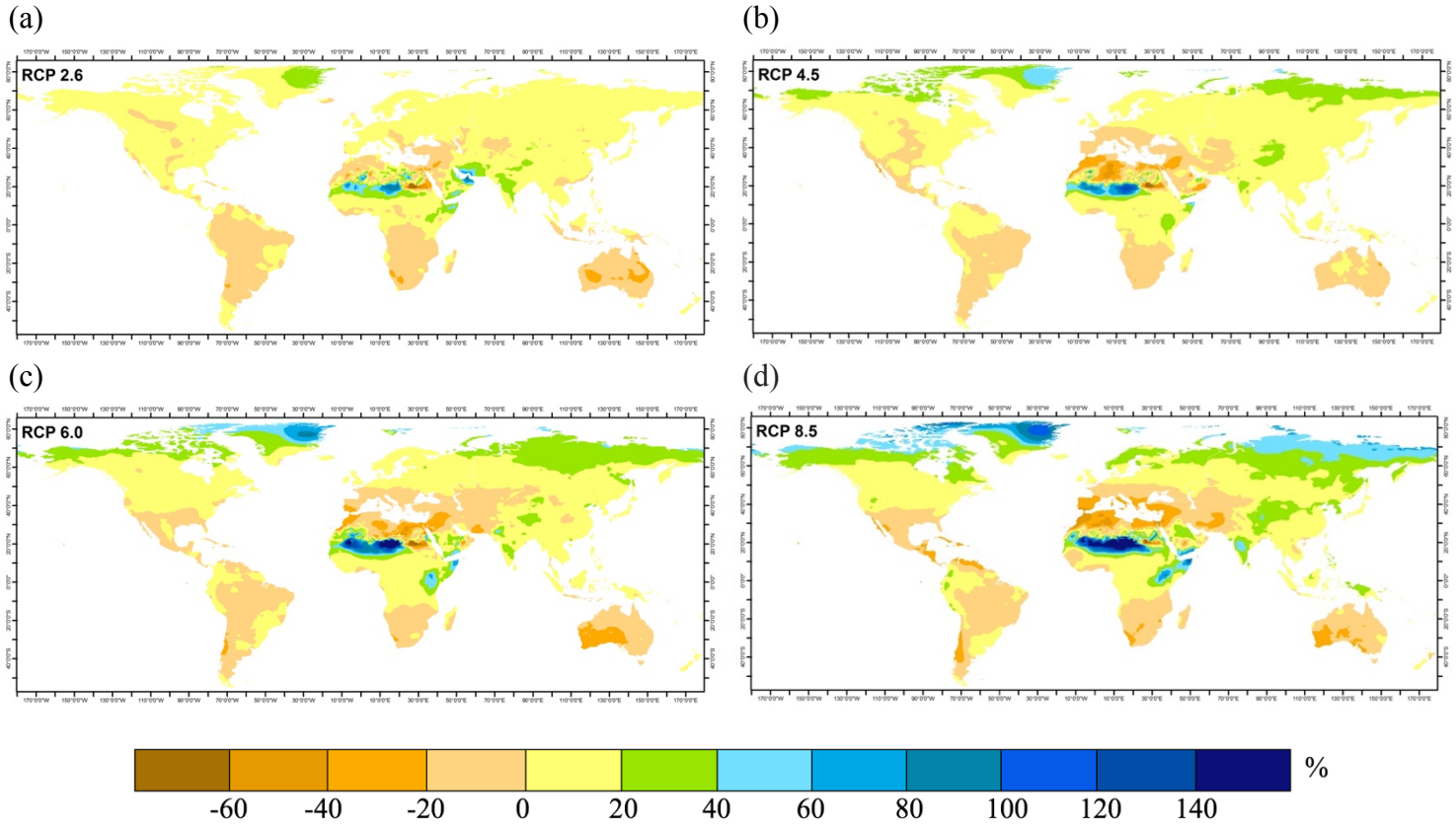

Figure 3: Change in global averaged precipitation based on the multi model ensemble projections for the last decade of the 21st century (2090-2099) relative to the first decade of the 21st century (2000-2010) under all RCP scenarios.

Figure 4 shows the decadal averages of mean global temperature and precipitation throughout the study period (1950-2099). Toward the end of the century both precipitation and temperature show an increase with increasing RCP scenario. However, at the beginning of the century the change in both variables is similar in the four RCPs, and by the mid 21st century, the magnitude of the projected change increasingly deviates for each RCP. Similar trends have also been reported in IPCC (2014).

(a) (b)

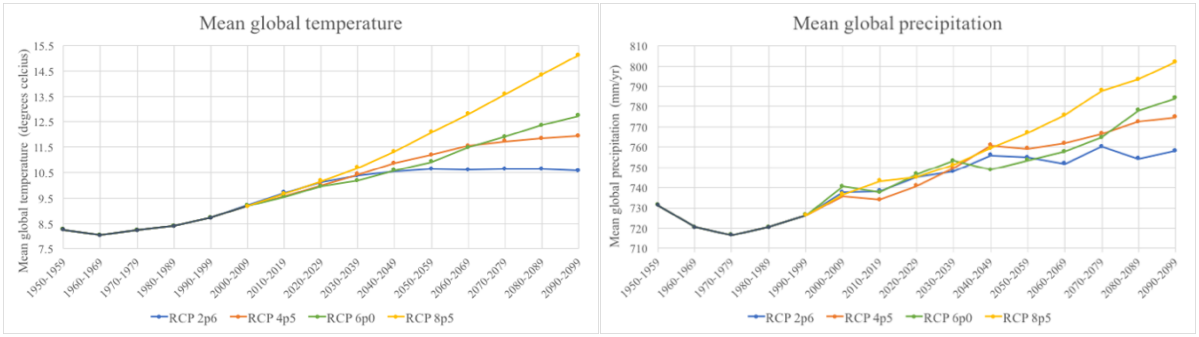

Figure 4: Mean global temperature (a) and mean global precipitation (b) for each decade under each RCP scenario based on the multi model ensemble projections.

3.3 21st century changes in river discharge and sediment dynamics at a global scale

Considerable changes in river discharge (Figure 5) and suspended sediment loads (Figure 6) can be observed in large global rivers toward the last decade of the 21st century relative to the present decade under projected changes in climate. River discharges are predicted to increase in the Arctic, north and east Africa, south and east Asia, and some parts of North America with increasing GHG-induced warming (Figure 5). Decreases in river discharges are projected for southern and western Europe, some pats in central Africa, central and middle east Asia, much of north America and south America, and Australia. These changes are broadly consistent with other studies that have examined the global scale response of river discharge to climate change

(Arnell, 2003; Milly et al., 2005; Nakaegawa et al., 2013; Schewe et al., 2014; Sperna Weiland et al., 2012).

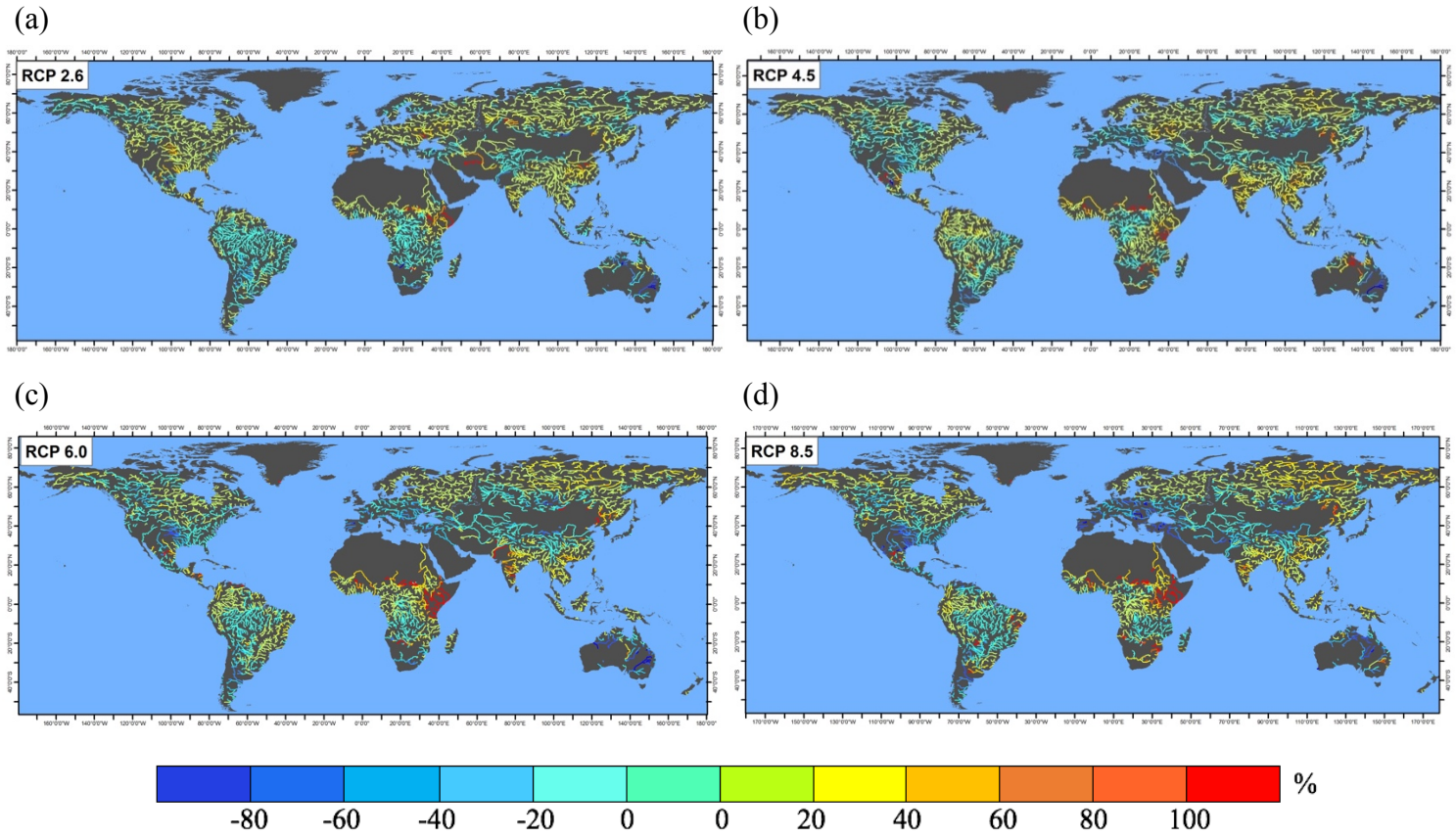

Figure 5: Percentage difference in global river discharge between the present decade and the last decade of the 21st century between RCP scenarios based on the ensemble. Predictions are presented only for grid cells with a contributing area > 10,000 km^2 and long-term average discharge > 30m^3/s.

Changes in sediment flux closely corresponds to the patterns in discharge (Figure 6). However, since the relationship between discharge and sediment flux is nonlinear in space and time, both in the model and in reality (Vercruysse et al., 2017), the response of sediment flux to global climate change cannot be quantified based on discharge dynamics alone. For example, in east Asia, increase in sediment is larger than that of discharge (Figures 5 and 6). This may be due to the role, lithology plays in this area (Syvitski et al., 2005).

In most parts of the world these changes in discharge and sediment flux are closely related to projected future changes in global distribution of precipitation (Hagemann et al., 2013; Syvitsky et al., 2005; Zhu et al., 2008). In the Nile river basin, although precipitation shows a decreasing trend toward the outlet, larger increases in precipitation are evident in the southern parts of the basin in all RCP scenarios (Figure 3). The influence of basin wide precipitation patterns for discharge and sediment can be seen for the Nile in all RCP scenarios by the increases predicted for discharge and sediment flux toward the outlet. It is also evident that with increasing warming scenarios, the number of rivers that will experience larger changes (either increasing or decreasing) in both discharge and sediment flux can be expected to increase. Other studies such as Coulthard et al. (2012), Hirabayashi et al. (2008) also found a similar trend.

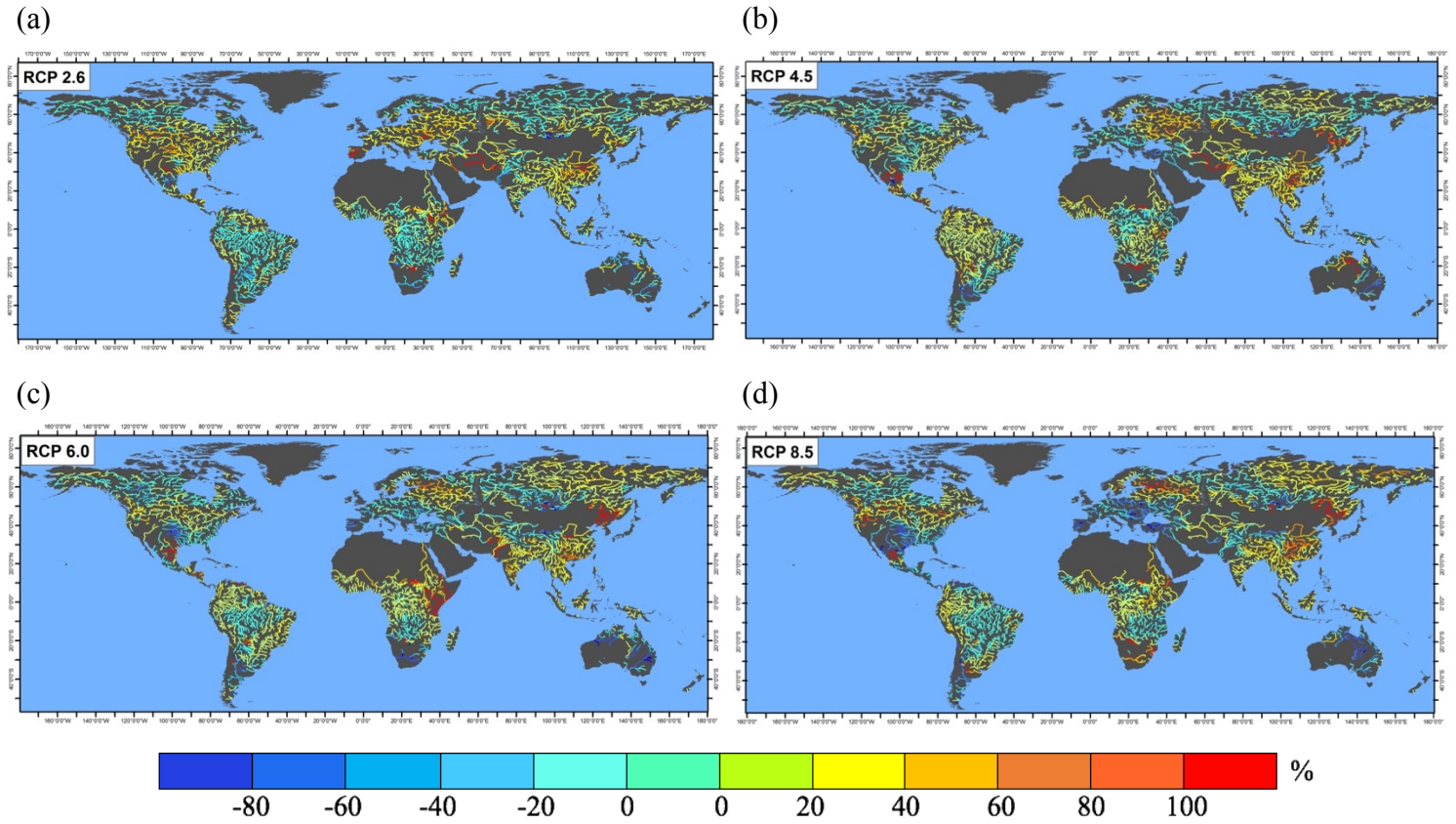

Figure 6: Percentage difference in global riverine suspended sediment flux between the present decade and the last decade of the 21st century between RCP scenarios based on the ensemble. Predictions are presented only for grid cells with a contributing area > 10,000 km^2 and long-term average discharge > 30m^3/s.

The changes in global mean river discharge and sediment flux in the last decade relative to the present decade of the 21st century are presented in Table 1. Despite regional differences, at a global scale, both discharge and sediment flux show a net increase at the end of the 21st century with all RCP scenarios. The increases are generally larger with increasing RCP. An overall increase in river discharge at a global scale in response to climate warming are also reported in other studies (Hirabayashi et al., 2008; Sperna Weiland et al., 2012). The increase in sediment flux is greater than that of discharge in all RCP scenarios.

Table 1: Percentage difference in global mean river discharge and sediment flux in the last decade relative to the present decade of the 21st century in all RCP scenarios.

% difference in the last decade relative to the present decade	RCP 2.6	RCP 4.5	RCP 6.0	RCP 8.5
Mean global river discharge	1.05	5.64	5.02	7.33
Mean global sediment flux	5.05	6.93	9.07	14.7

Figure 7 shows the decadal averages of total river discharge and sediment flux to global oceans from major river outlets throughout the simulation period. Temporal trends in fluvial fluxes to the oceans correspond well with global patterns in temperature and precipitation (Figure 4), but with much more dramatic fluctuations. This demonstrates the complex relationship between precipitation and discharge at a global scale, and justifies the need to use a model, as precipitation cannot be used alone to quantify future trends in discharge or sediment flux.

A clear increase in discharge and sediment flux to the global oceans is predicted toward the end of the 21st century with increasing RCP. In accordance with the trends in precipitation, RCP 4.5 and 6.0 moderate warming scenarios, generate the largest discharge and sediment flux

at a global scale in the mid-century. However, interestingly, the hindcast simulations for discharge and sediment flux also shows high values in the 1950's, due to high precipitation amounts (Figure 4b).

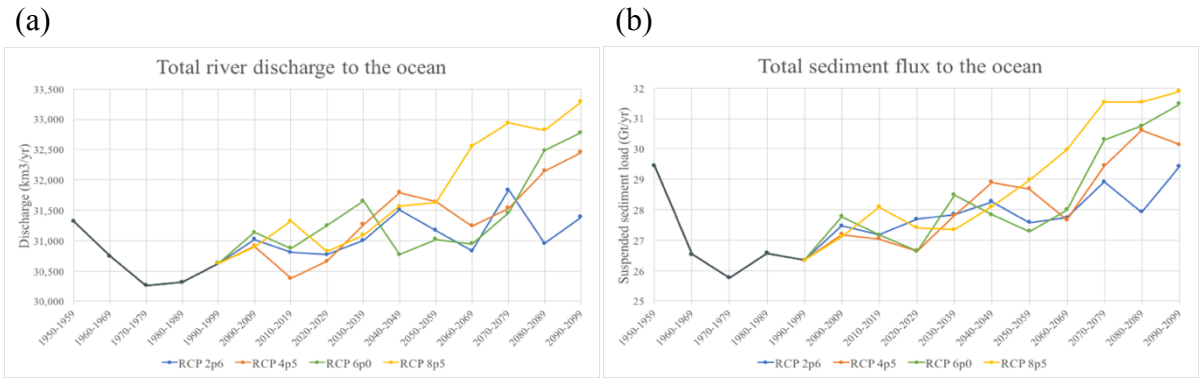

Figure 7: Total global river discharge (a) and suspended sediment flux (b) to the ocean from major river outlets in the world (river outlets with > 10,000 km^2 drainage area and > $30m^3/s$ long-term average discharge) for each decade based on the ensemble.

Averaged by continent, Asia and Africa will experience increases in discharge and sediment flux toward the end of the century under all RCP scenarios (Table 2). North America will have increasing discharge and sediment flux for low and moderate warming, but for RCP 8.5 both discharge and sediment will decrease by the end of the 21st century, due to considerable precipitation decreases in the south of the continent (Figure 3) and decreasing discharge in the snow-dominated western part of the Mississippi Basin (Figure 5). In the continental South America, only moderate RCP scenarios will have increasing sediment and water discharge. However, RCP 8.5 will also have increasing sediment flux despite the decrease in discharge. All scenarios except the low warming one will lead to lower sediment and river discharge in Europe toward the end of the century. In Australia, all the warming scenarios will lead to decreased discharge and sediment flux, with the exception of RCP 4.5 with a percentage increase in discharge. Contrasting trends are projected in sediment and discharge in a number of rivers. This

counterintuitive contrast is due to a number of factors including the dependency of sediment on the interaction between climate and other factors such as lithology, relief etc. (Ludwig and Probst, 1996), an artifact of mathematical averaging of simulation results to create ensembles, and/or the way temporal sediment dynamics are calculated in the model. This will be further discussed in the Discussion section.

At a continental scale, largest percent increase in discharge is projected for Asia under RCP 8.5, while largest percent decrease is predicted for Australia (RCP 8.5). For sediment flux, largest percent increase was predicted for Europe (RCP 2.6) while largest percent decrease is in Australia (RCP 6.0). Inter-continental trends are quite complex with various rivers showing varying responses to future warming scenarios. A detailed analysis of how river discharge, sediment flux, basin-wide precipitation and basin-averaged temperature would change over time in selected eight major river outlets in the world for all RCP scenarios are presented in the appendix.

Table 2: Percentage change in the last decade relative to the present decade in sediment flux and discharge to the global oceans from continents and major river basins with > 10,000 km^2 drainage area and > $30m^3/s$ long-term average discharge. Significant changes (paired t-test, $p<0.05$) are indicated by *.

Continents and major river basins	Total number of river outlets	Total WBMsed land area draining to the ocean (x 10^6 km^2)	RCP 2.6		RCP 4.5		RCP 6.0		RCP 8.5	
			Discharge (%)	Sediment flux (%)	Discharge (%)	Sediment flux (%)	Discharge (%)	Sediment flux (%)	Discharge (%)	Sediment flux (%)
Asia	**164**	**26.08**	**7.09**	**15.2**	**12.8**	**20**	**14.6**	**27.56**	**17.8**	**26.25**
Ganges-Brahmaputhra		1.53	9.8*	14.2	18.2*	29.7*	16.9*	34.7*	19.8*	33.6*
Indus		0.86	-13.1	-26.3	8	38.6	2.33	34.3	-19.7*	-6
Yangtze		1.88	23.3*	53.65*	15.4*	46.6*	1.85	26	13*	63.12*
Yenisei		2.7	4.87	-3.14	9.4*	-3.68	16.4*	9.86	21*	3.5
Mekong		0.8	8.25	14.1	18.13*	26.05*	15.1*	26.03*	7.55*	14.5*
Lena		2.45	3.44	-0.27	11.44*	10.7	25*	29.5*	32.5*	36.5*
Irrawaddy		0.4	9.57*	12.1*	20.13*	27.1*	9.1*	12.8*	21.3*	30.7*
Yellow		0.91	8.39	58.8*	3.24	55	-14.35*	26.13	-13*	56.03*
Godavari		0.33	12	1.51	33*	26.2	36.84*	29.06	36.1*	21.8
Song Hong		0.14	0.73	3.62	33.68*	50.7*	27*	45.4*	20.2*	32.2*
Chao Phraya		0.14	16.6	16.17	47.33*	44.35*	29.7*	29.7*	30.2*	27.1*
Fly		0.06	-1.48	0.58	0.68	0.94	11.2*	15*	17.2*	20.3*
Africa	**84**	**18.45**	**1.39**	**5.94**	**4.57**	**3.83**	**11.8**	**25.85**	**12.57**	**19.38**
Congo		3.75	-3.63	-0.6	-2.7	-0.4	2.1	5.55	8.4*	15.3*
Nile		3.25	13.2	13.9	13.11	10.1	37*	40.6*	52.7*	45*
Niger		2.7	8.45	3.5	26*	26.4*	39.5*	38.1*	33.3*	31.6*
Orange		1	-28.33	-34.3	6.7	-3	-30.33	-63.8	25.5	57.1
Zambezi		2.09	-5.66	-4.2	-1.8	1.3	1.42	3.11	-11.02	-8.8
Jubba-Shebelle		0.53	67.42	31.23	31.32	-23.1	139.6*	88	131.7*	12.2
Senegal		0.66	17.43	9.37	56.55*	42.2*	48.2*	28.9	29.6*	11
Europe	**69**	**5.58**	**5.83**	**31.34**	**-3.57**	**-7**	**-5.12**	**-18.74**	**-10.6**	**-33.8**
Danube		0.82	6.4	26.03*	-24*	-17.2	-25*	-22.22*	-42.8*	-43.8*
Meuse		0.04	4.73	11.18	-12*	-4.43	-14.7*	-8.44	-24.6*	-16.7*
Rhone		0.1	8.73	25.78*	-17.5*	0.21	-25.1*	-18.2*	-38*	-26.7*
Po		0.07	14.68*	35.06*	-20.5*	-8	-24.2*	-17.03	-37.9*	-27.6*
Australia	**28**	**3.57**	**-18.59**	**-10.74**	**13.3**	**-8.33**	**-24**	**-38**	**-27.6**	**-32.45**
Murray-Darling		1.06	-24.04	-26.04	-43	-52	-54*	-53.8	-36.5	-26.6

N. America	**149**	**16.11**	**7.66**	**17.56**	**3.04**	**13.85**	**0.62**	**4.11**	**-2.18**	**-12.4**
Mississippi		3.26	11.18	26.35*	-5.83	5.45	-8.7	-1.1	-20.6*	-11.3
Rio Grande		0.62	-12.22	-25.5	43.28	184	20.6	78.4	-44.4	-54.8
Columbia		0.72	9.8	39.03*	0.24	32.25*	1.92	37.5*	0.03	42.6*
Colorado		0.7	6.34	21.44	-14.93	-4.83	-10.2	0.82	-33.4*	-31.4*
Mackenzie		1.77	.91	-6.86	3.2	-4.65	-0.86	-10.4	9*	-5.8
Nelson		1.14	7.27	38.77*	-1.4	24.18*	3.25	24.2*	0.94	30.2*
S. America	**81**	**15.11**	**-4.2**	**-2.2**	**5.47**	**8.18**	**0.3**	**4.89**	**-1.07**	**2.7**
Amazon		5.34	-5.56	-4.2	6.65*	15.7*	-2.4	0.55	0.96	4.6
Orinoco		0.93	2.34	3.58	11.6	19.1	5.8	11.02	-7.6	-9.1
Parana		3	-6.25	-2.31	-5.67	-5.74	3.65	10.92	-6.8	1.5
Magdalena		0.27	9.45	10.2	27.2*	42.6	24.1*	29.5*	14.6*	14.7
Tocantins		0.76	-8.67	-6	-1.71	2.87	0.4	1.0	-5.9	-4.5

3.4 Significant trends in discharge and sediment fluxes

The pixel-wise Mann-Kendall trend test was performed for the time series of ensemble model outputs in each RCP scenario to identify grid-cells that have significant increasing or decreasing trends. This showed that, as warming increases, more significant trends (either increasing or decreasing) in both discharge and sediment can be expected toward the end of the 21st century (Figure 8). At a global scale, the number of pixels that resulted in statistically significant ($p<0.05$) increasing trends in both discharge and sediment flux will increase with increasing RCP scenarios (Table 3). Also, the number of pixels that resulted in significant decreasing trends ($p<0.05$) in the two variables will also increase with increasing RCP scenarios. However, for a given variable, the number of pixels that will experience significant increasing trends are greater than those of significant decreasing trends for all RCP scenarios.

In south-east Asia, some parts of Europe, and parts of Africa, the increasing trends in both discharge and sediment flux in response to climate change will be significant in all RCP scenarios (Figure 8). In high latitudes of the northern hemisphere and western regions of South America, significant increases in both variables can be seen with moderate and high warming scenarios. In North America, most of the significant increasing trends in both variables are predicted under low and high warming scenarios. This means that, a significant monotonic increasing trend in discharge and sediment flux can be expected in these regions over the 21st century due to climate warming. In contrast, south and central regions of Europe, some regions of Asia, southern regions of North America, central America, southern regions of Australia, and southern regions of South America will experience significant decreasing trends in both variables under moderate and high RCP scenarios.

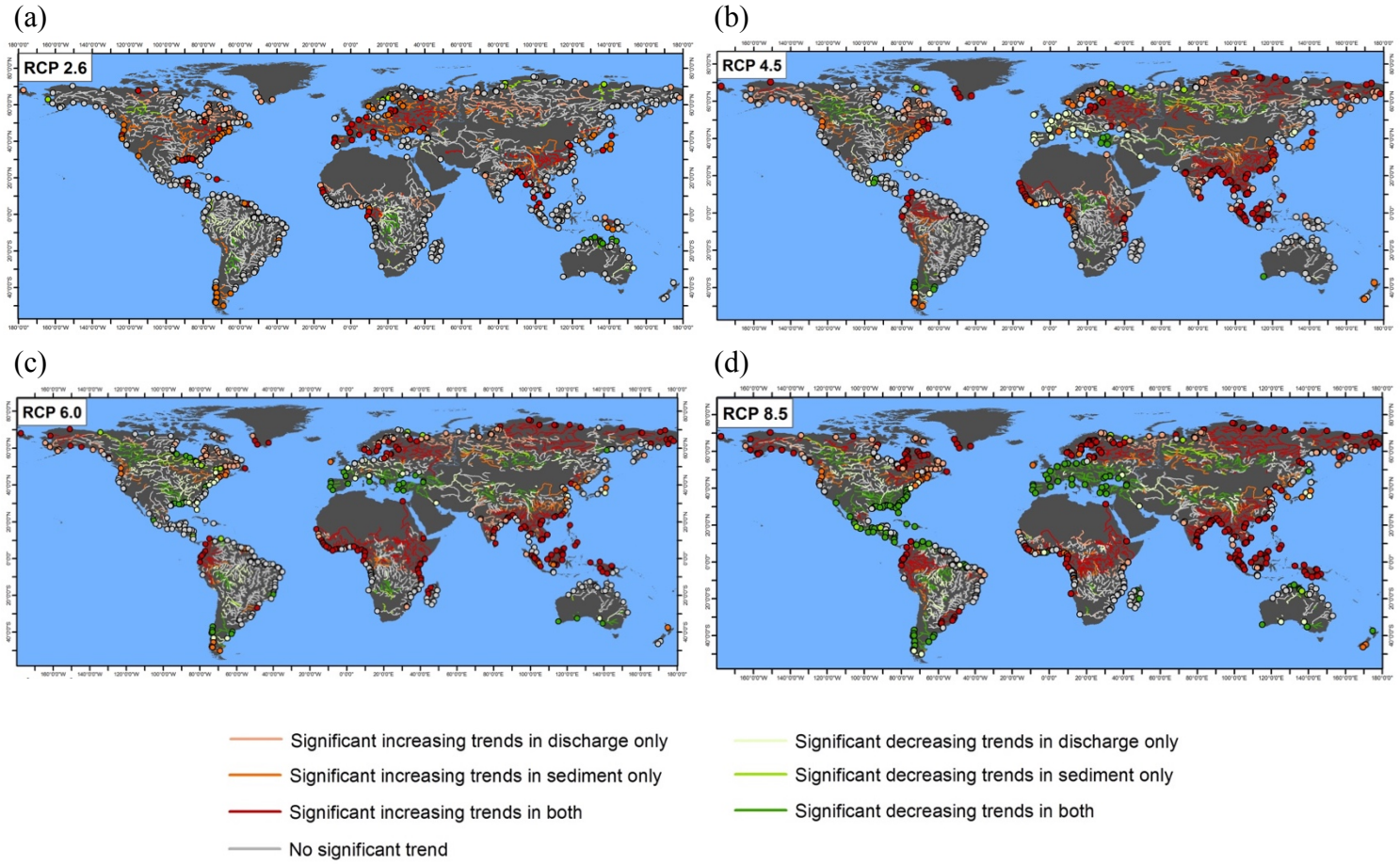

Figure 8: Pixel-wise Mann-Kendall trend analysis of discharge and sediment flux between 2006 – 2099 in each RCP scenario based on the ensemble. Predictions are presented only for grid cells with a contributing area > 10,000 km^2 and long-term average discharge > 30m^3/s.

Table 3: Percentage grid cells that will experience statistically significant trends (Mann-Kendall trend test, $p<0.05$). Calculations are based only on grid cells with a contributing area > 10,000 km^2 and long-term average discharge > 30m^3/s.

% grid cells with statistically significant trends	RCP 2.6	RCP 4.5	RCP 6.0	RCP 8.5
Increasing both discharge and sediment flux	9.01	17.91	21.46	30.31
Increasing discharge	18.6	30.51	30.21	37.82
Increasing sediment flux	19.13	27.06	29.07	38.6
Decreasing both discharge and sediment flux	2.08	4.55	9.97	14.65
Decreasing discharge	7.43	12.81	22.04	25.52
Decreasing sediment flux	4.85	9.31	13.18	18.07
Overall significant trends in discharge	26.03	43.33	52.25	63.34
Overall significant trends in sediment flux	23.97	36.36	42.24	56.66

In addition, the river segments in the world that will experience statistically significant trends in river discharge and sediment flux with any given RCP scenario was created (Figure 9). Whichever warming scenario the planet will experience, these river segments will have significant changes in discharge and sediment flux in response to climate. This includes rivers in south-east Asia, northern regions of Europe, western Africa, and northern regions of North America. These can be considered as hotspots that will be affected by any of the future RCP scenarios. Therefore, these areas are more sensitive to climate changes and needs special attention when managing rivers and formulating climate change adaptation strategies.

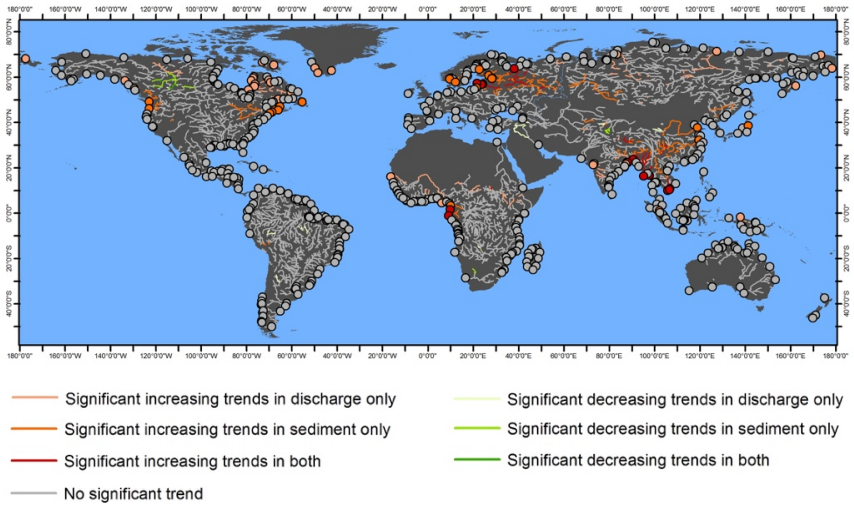

Figure 9: Global rivers which will experience significant trends in discharge and sediment flux in the 21st century with any given warming scenario. Predictions are presented only for grid cells with a contributing area > 10,000 km^2 and long-term average discharge > 30m^3/s.

3.5 Variability in future discharge and sediment flux

The non-stationarity in future climate is predicted to increase in the future with increasing levels of climate change (IPCC, 2014; Krakauer and Fekete, 2014; Pendergrass et al., 2017). Changes in temporal dynamics of fluvial fluxes can considerably affect the hydrologic, geomorphic, and ecological functioning and regimes of a river system (Walling and Fang, 2003). It is therefore important to assess the temporal variability in future river discharges and sediment fluxes induced by climate change. Temporal variability, evaluated by calculating CV, shows that inter-annual variability in both river discharge and sediment flux increases with increased GHG-induced warming (Figures 10 and 11), in agreement with other studies (e.g. Arnell, 2003). The patterns in inter-annual variability in discharge coincide with that of sediment flux, however the magnitude of the variability differ between the two variables (Figures 12 and 13). The number of grid cells that will experience increases in inter-annual variability in discharge relative to RCP 2.6, is greater than that of sediment flux in all warming scenarios (Table 4 and 5).

Inter-annual variability in discharge and sediment flux are larger in Australia, southern and eastern Africa, central parts of North America, central and eastern parts of South America, middle eastern Asia and some parts of Europe (Figures 10 and 11). In contrast, less inter-annual variability in river discharge and sediment flux can be expected in south east Asia, high latitudes of Northern Hemisphere, eastern parts of North America, northern Europe, central Africa and central South America (Nijssen et al., 2001).

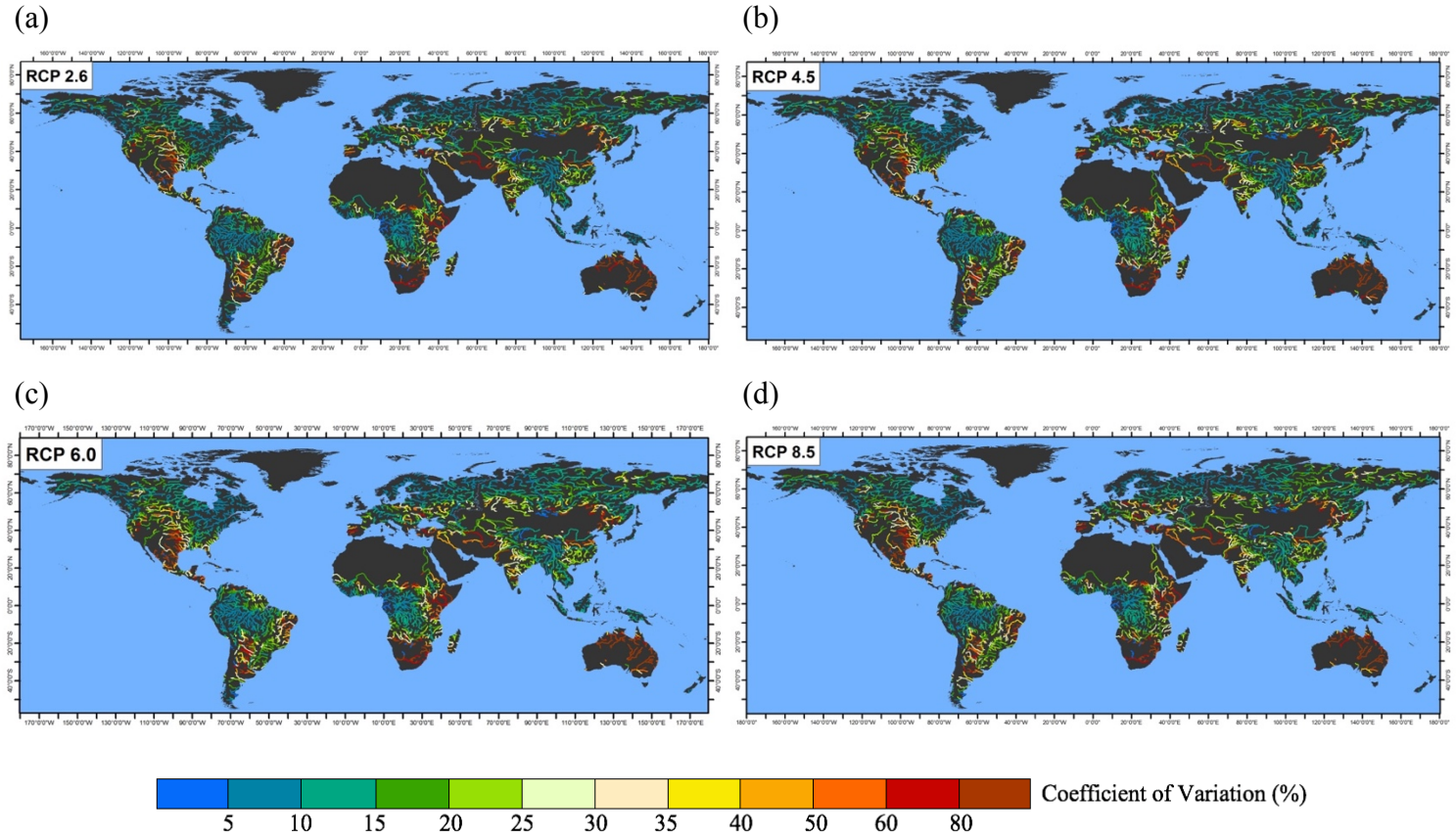

Figure 10: Inter-annual variability in discharge during the 21st century between RCP scenarios based on the coefficient of variation (CV). Predictions are presented only for grid cells with a contributing area > 10,000 km^2 and long-term average discharge > 30m^3/s.

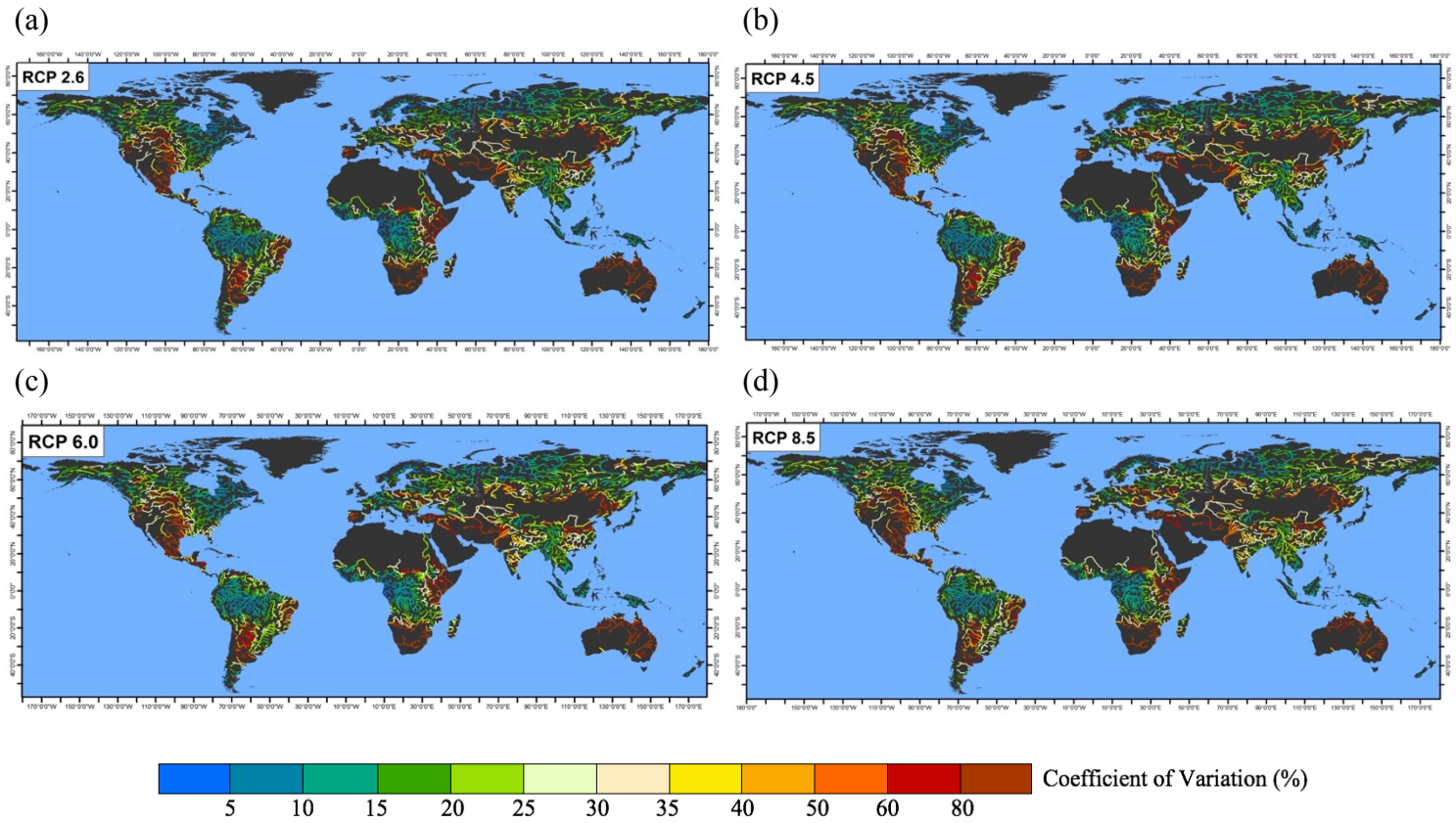

Figure 11: Inter-annual variability in sediment flux during the 21st century between RCP scenarios based on CV. Predictions are presented only for grid cells with a contributing area > 10,000 km^2 and long-term average discharge > 30m^3/s.

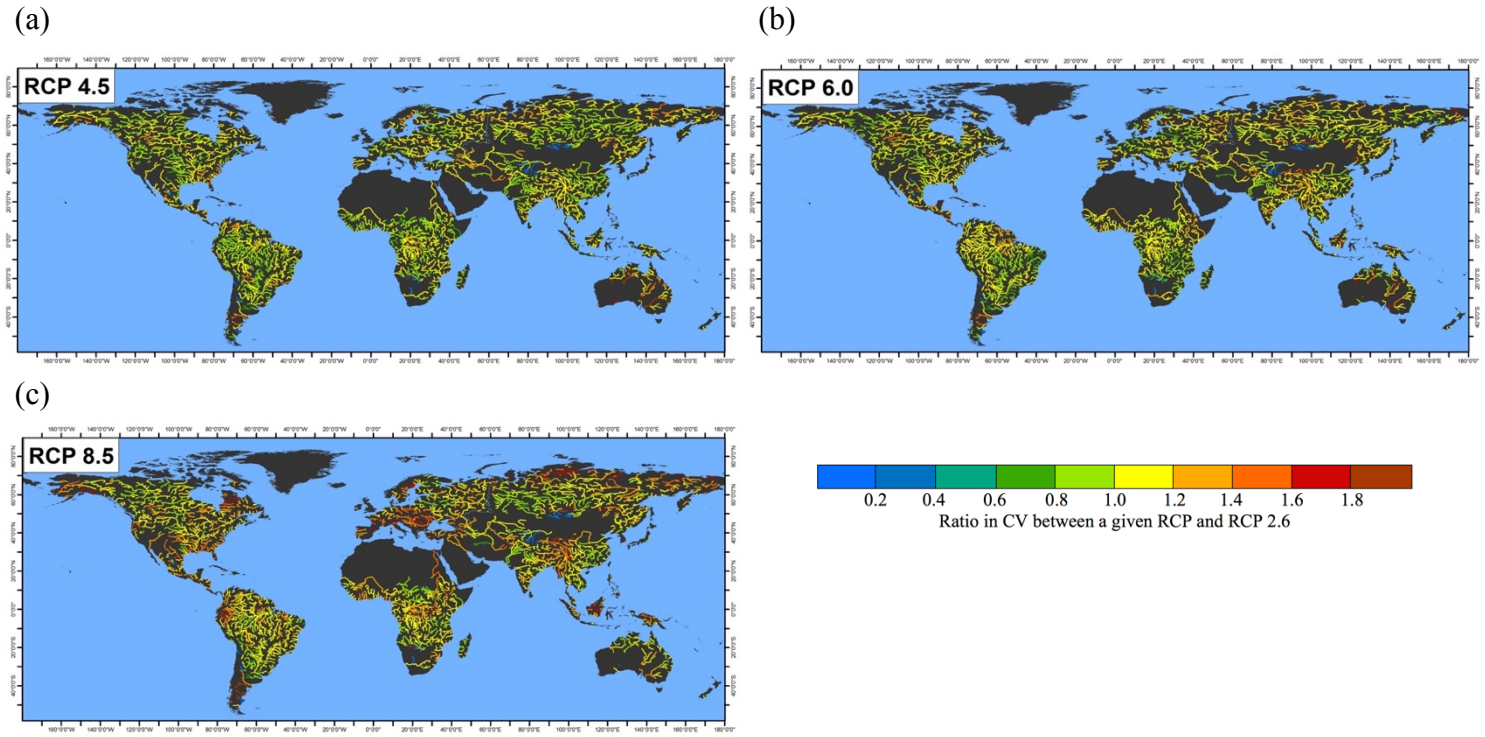

Figure 12: The change in CV in river discharge between RCPs relative to RCP 2.6. Predictions are presented only for grid cells with a contributing area > 10,000 km^2 and long-term average discharge > 30m^3/s.

Table 4: Percentage of grid cells with ratio in CV between a given RCP scenario and RCP 2.6 for river discharge. Calculations are based only on grid cells with a contributing area > 10,000 km^2 and long-term average discharge > 30m^3/s.

Ratio in CV between a given RCP and RCP 2.6	RCP 4.5	RCP 6.0	RCP 8.5
< 1.0*	43.22	32.85	21.78
> 1.0**	56.78	67.14	78.25

*Indicate low inter-annual variability relative to RCP 2.6
**Indicate high inter-annual variability relative to RCP 2.6

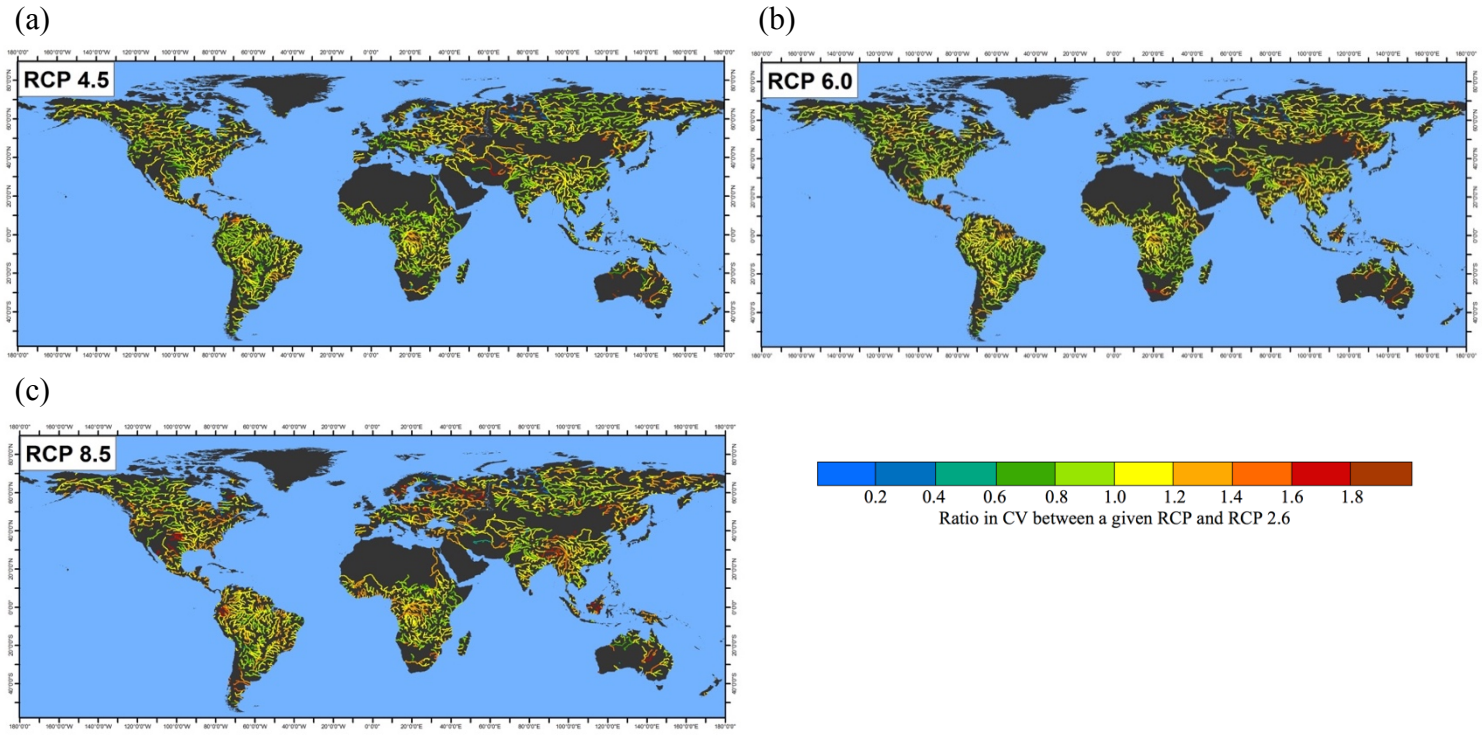

Figure 13: The change in CV in sediment flux between RCPs relative to RCP 2.6. Predictions are presented only for grid cells with a contributing area > 10,000 km^2 and long-term average discharge > 30m^3/s.

Table 5: Percentage of grid cells with ratio in CV between a given RCP scenario and RCP 2.6 for sediment flux. Calculations are based only on grid cells with a contributing area > 10,000 km^2 and long-term average discharge > 30m^3/s.

Ratio in CV between a given RCP and RCP 2.6	RCP 4.5	RCP 6.0	RCP 8.5
< 1.0*	49.65	46.04	30.60
> 1.0**	50.36	53.96	69.40

*Indicate low inter-annual variability relative to RCP 2.6
**Indicate high inter-annual variability relative to RCP 2.6

Change in discharge and sediment flux and their variability between latitudinal regions, are shown for both global rivers and river outlets, in Figures 14 and 15 respectively. Global river discharge (Figure 14a) is highest around the equator, but sediment flux (Figure 14b) is highest in 25º N latitude closely followed by equatorial regions.

In discharge, inter-annual variability increases with increasing warming scenario in most of the latitudinal regions (Figure 14c). For sediment flux, moderate warming scenarios and low warming scenario have higher inter-annual variability in some regions (Figure 14d). For e.g. 35º - 40º N and also equatorial regions show high inter-annual variability in sediment flux for low and moderate RCPs. High variability in both discharge and sediment can be seen in southern mid-latitudinal regions. It is interesting to note that variability in discharge does not always mean variability in sediment flux. This also demonstrates the complex and nonlinear relationship between discharge and sediment flux in rivers.

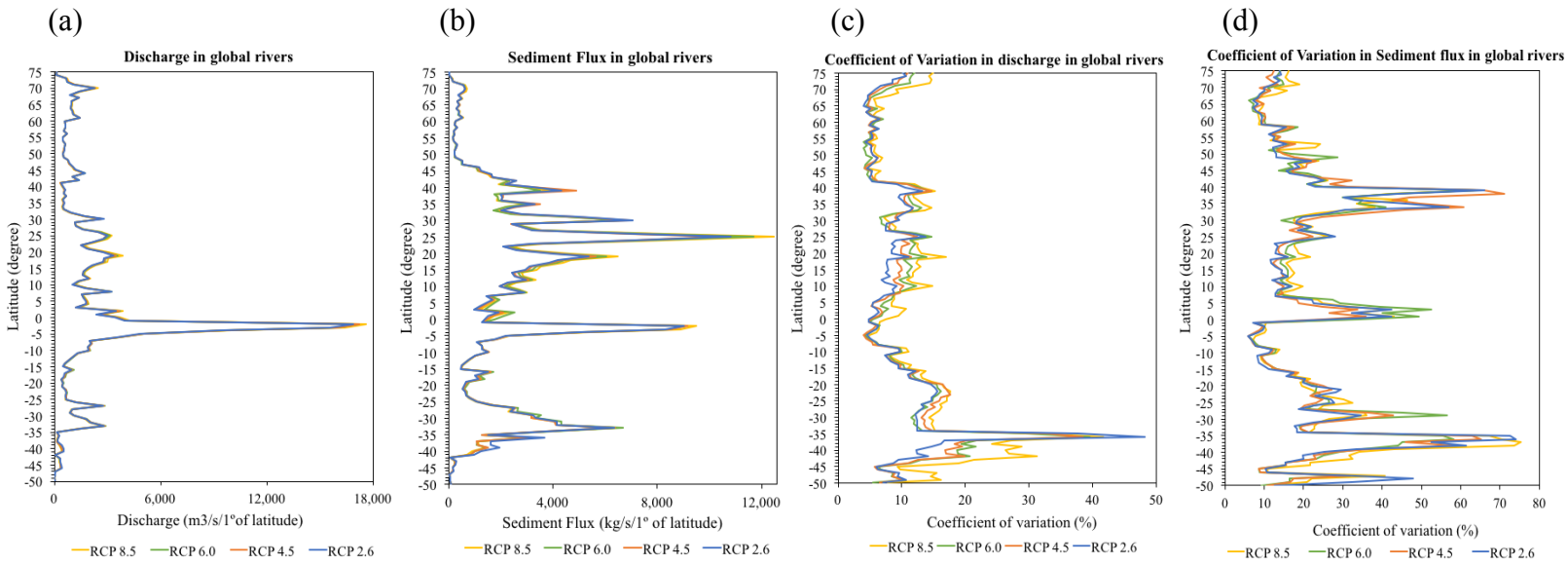

Figure 14: Change in long-term average global river discharge (a), sediment flux (b), CV in discharge (c), and CV in sediment flux (d) between latitudinal regions for the period between 2010-2099. Values averaged across 1 degree of latitude, for only grid cells with a contributing area > 10,000 km^2 and long-term average discharge > 30m^3/s.

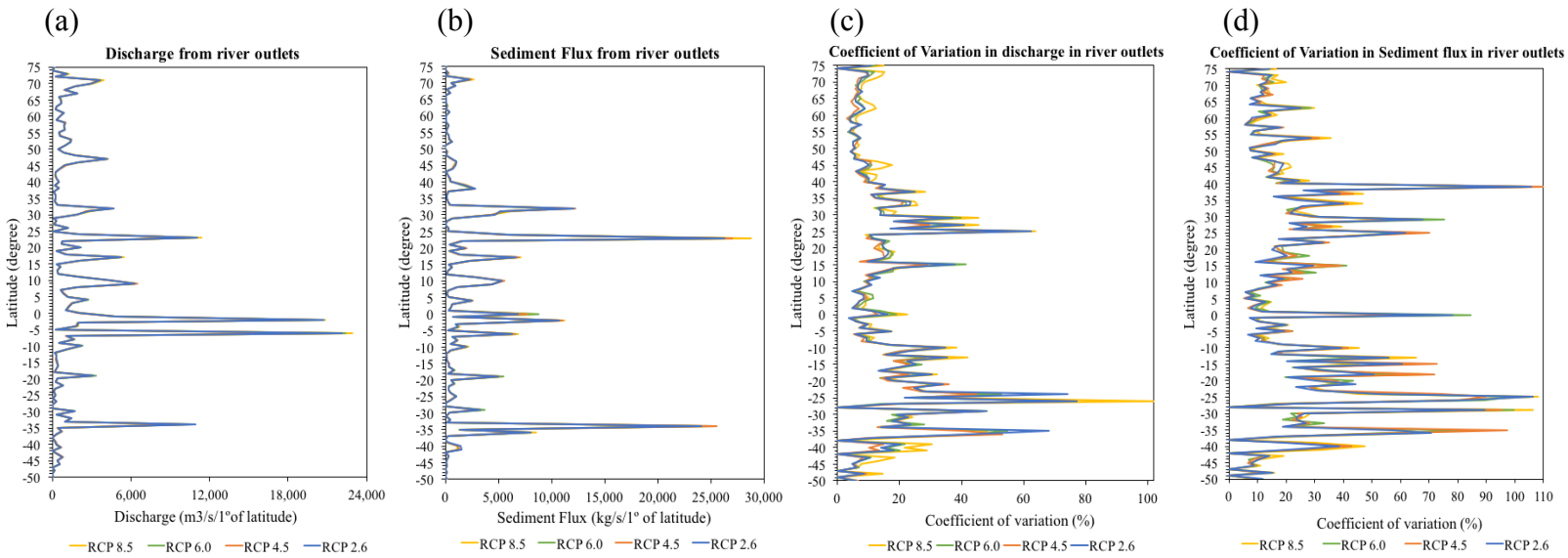

Figure 15: Same as figure 14, but for fluxes to the global ocean from river outlets with a contributing area > 10,000 km^2 and long-term average discharge > 30m^3/s.

CHAPTER 4

DISCUSSION

Due to the different structures and parameters used in GCMs, future projected changes in temperature and precipitation have large spatial and temporal uncertainties even for the same radiative forcing levels (Cai et al., 2009; Knutti and Sedláček, 2013). Therefore, studies that investigate climate change responses of fluvial systems show varying degrees and directions of changes over the 21st century in river discharge and sediment flux (Arnell, 2003; Haddeland et al., 2014; Hagemann et al., 2013). These discrepancies are partly due to the number of GCMs used to generate predictions for global river discharge and sediment loads in different catchments in the world. Some studies have used only one GCM (Nakaegawa et al., 2013), while some studies were done using as high as 19 GCMs (Nohara et al., 2006). Therefore, the use of multi-model ensemble is advised in many studies (Haddeland et al., 2014; IPCC, 2014, Milly et al., 2005; Nijssen et al., 2001). Here I used five ISI-MIP models to obtain future temperature and precipitation projections which were used as input to the WBMsed global-scale hydro-geomorphic model, and the predicted changes in discharge and sediment flux were averaged for all GCMs to generate yearly ensembles. Future discharge and sediment flux projections generated by these ensembles for the four RCP scenarios were generally consistent with most previous studies. However, direct comparisons are difficult to be made in part due to the differences in climate change scenarios used and different variables simulated in those studies.

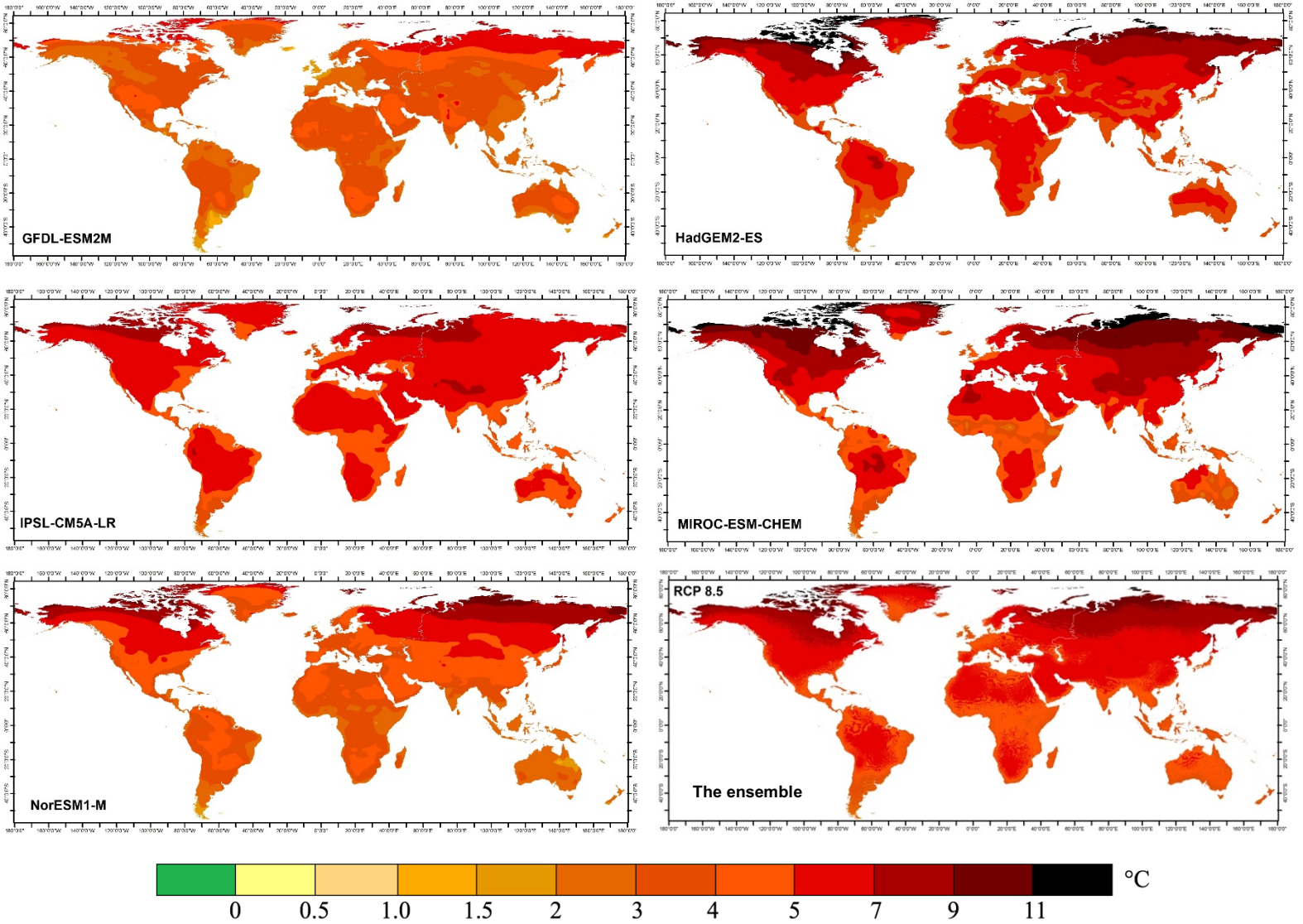

Figure 16: The spread of individual GCMs for global averaged land surface temperature projections for the last decade relative to the first decade of the 21st century under RCP 8.5 scenario.

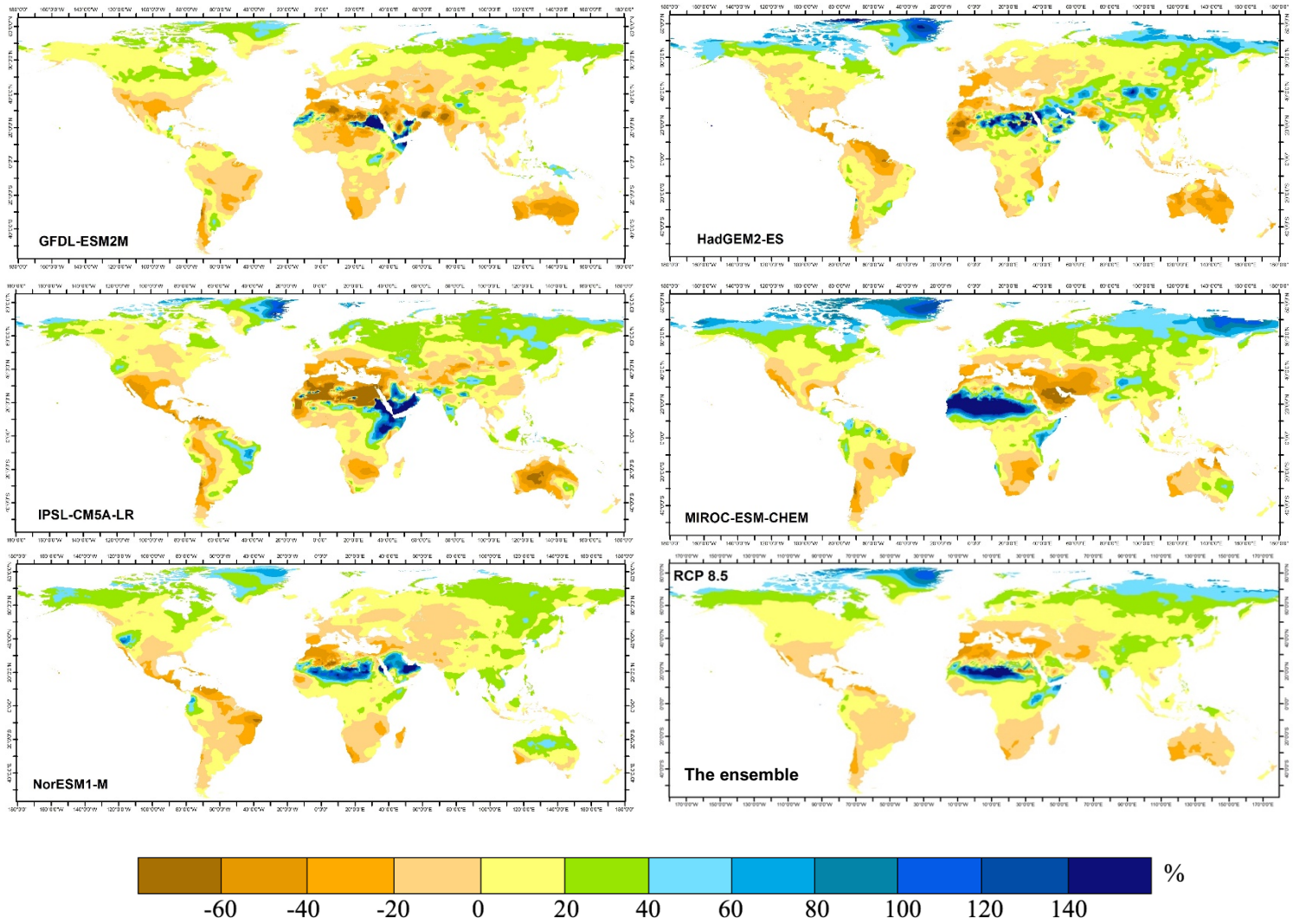

Figure 17: The spread of individual GCMs for global averaged precipitation projections for the last decade relative to the first decade of the 21st century under RCP 8.5 scenario.

It should also be noted that by averaging the results of multiple GCM projections to create the ensembles, extremes are reduced and changes become less pronounced (Materia et al., 2010). When considering the time series of sediment flux and discharge for a given river (Figures 16 –23 in the appendix), much larger extremes can be seen by individual GCMs, whereas they are smoothened in the ensemble which was used in this analysis. The analysis also shows a considerable spread in the individual GCM results (Figures 16 and 17). It is also interesting to note that in some instances, the individual GCM based projections are not consistent with the direction of change in the ensemble. This is due to the changes in GCM structure and parameterization as discussed previously that resulted in different precipitation distribution patterns in response to warming. Considerable differences between individual GCM predictions and contrasting trends are reported widely in the literature (Arnell, 2003; Haddeland et al., 2014; Hagemann et al., 2013; Schewe et al., 2014; van Vliet et al., 2013) and some have attributed this to the discrepancies in precipitation distribution predicted by these climate models (Covey et al., 2003; Krakauer and Fekete, 2014). Hence, the use of the multi-model ensemble is justified, where the ensemble leans toward the major direction of change as predicted by most number of GCMs. However, there are instances where one or two GCMs dominate the direction of change due to their high magnitude of discharge and sediment flux predicted. One such example is the Nile river (Figure 21 in the appendix), where the trend in the ensemble is mostly affected by one of the GCMs (IPSL-CM5A-LR) that dominates the direction of change.

In this study, a non-weighted ensemble of the five GCMs was used for the trend and variability analysis. However, depending on the model sensitivity, fit of individual GCMs with observational values for the hindcast period, and differences in model uncertainties associated with each GCM, a different approach to create the model ensembles may provide more robust

results. One such approach is the Bayesian Model Averaging (BMA), which can be used to statistically combine each GCM based WBMsed model simulations for separate RCP scenarios, depending on their fit with observed data. It assigns weights for each GCM based model simulation and calculates the value for the BMA probability distribution, which can also be used to quantify the range of uncertainty associated with the model ensemble predictions. This approach will be considered in future work.

While the use of GCM projections of future climate are a major source of uncertainty (Teng et al., 2012), there are other sources of uncertainties associated with this study. The range of changes in future climate conditions that can be captured by ISI-MIP climate models may have limitations, and thereby introduce some uncertainty to the study. McSweeney and Jones (2016) evaluated the range of change in future climate that can be captured by the ISIMIP subset relative to the CMIP5 full ensemble of 36 GCMs. They showed that the fraction of the full range of future climate across different regions and seasons that can be captured by the ISIMIP subset varies between 0.5-0.9 for temperature and between 0.3-0.8 for precipitation. However, this subset of five GCMs is widely used in climate change impact assessment studies and accounts for climate impacts in different sectors (such as water, biomes, agriculture, health and infrastructure; ISIMIP, 2019). Another source of uncertainty comes from the future GHG concentration scenarios, as they mimic a wide range of possible changes in future GHG concentrations based on a number of assumptions (Bjørnæs, 2013). In addition, the WBMsed model accuracy and simulation settings also introduce biases to this analysis as quantified in the validation procedure. The WBMsed model explicitly implements the already calibrated BQART equation in it. However, Cohen et al. (2013) suggests that a recalibration of the BQART equation based on the explicit WBMsed parameter calculations may improve the correlation between

simulated and observed long-term averaged sediment load values. Therefore, a part of the model related uncertainty associated with this study may be attributed to the calibration status of the model.

In this study, two hypotheses were tested. H1 states that increased GHG concentrations, represented by the four RCP scenarios, will lead to increases in the magnitude and variability in water discharge and fluvial sediment fluxes at a global scale. The results strongly support this hypothesis. The magnitudes of change evaluated by decadal percentage differences (Figure 5, 6) and total global river discharge and sediment flux to the ocean (Figure 7) clearly show that increases in river discharge and sediment flux in the 21st century can be expected with increasing levels of GHG concentrations in the atmosphere. In addition, the rivers that will experience statistically significant (Mann-Kendall, $p<0.05$) increasing trends in both discharge and sediment flux increase with increasing RCP scenarios (Table 3). Inter-annual variability, assessed by CV, showed that variability in both river discharge and sediment flux also increases with increased GHG-induced warming (Figures 10, 11, 12, 13).

The second hypothesis (H2) states that climate-induced temporal variability in suspended sediment fluxes and water discharge into global oceans is larger in tropical and higher latitudes than mid latitudes for a given RCP scenario. The results do not support this hypothesis. Figure 15 shows that both discharge and sediment flux do not show much variability in the arctic region. Inter-annual variability in discharge is large in the tropical region in both Northern and Southern hemispheres while the mid-latitudes of the Southern region also shows a large variability. Sediment flux variability is largest in the mid-latitudes in both hemispheres as well as around the equatorial region. However, inter-annual variability in discharge and sediment flux does not show a link to the changes in inter-annual variability in precipitation. Although precipitation

patterns mainly drive the changes in discharge and sediment flux, due to their nonlinear linkages, a particular precipitation event, for example, may exponentially amplify water discharges and sediment loads depending on the characteristics of the event (Coulthard et al., 2012). Changes in CV are mostly influenced by changes in the magnitudes of the high and low years of discharges and sediment fluxes throughout the study period (Arnell, 2003).

The sediment loads in rivers are mostly driven by water discharge. However, when the changes in the two variables between the last and the present decade are considered (Table 2), contrasting trends in discharge and sediment flux have been predicted in some rivers. One reason for this can be the discrepancies that arise by averaging out of the varying degrees of responses of individual GCMs when generating the ensemble. Another explanation to this could be the effects of the Psi equation (see Eq. 3 in the methodology) that is used in the model to calculate daily suspended sediment flux ($Q_{s_{[i]}}$), as a function of $Q_{[i]}/\overline{Q}$. The $C_{(a)}$ rating coefficient of this relationship is calculated as a function of R, that vary spatially, and $\overline{T}$, that vary both spatially and temporally. The yearly outputs generated by the model are based on averaging of the $Q_{s_{[i]}}$, so are the decadal averages. Therefore, the intra-annual variability in discharge and sediment flux largely controls the yearly outputs. This can create contrasting trends in decadal averages of discharge and sediment fluxes. This phenomenon will be further investigated in the future by analyzing daily model predictions.

Precipitation and temperature are the main driving forces of discharge and sediment flux in most hydrologic models when assessing the influence of climate (Syvitsky et al., 2005). Cohen et al. (2014) showed that while spatial and temporal variation in precipitation may have a major effect on discharge and thus sediment dynamics, other factors such as relief and lithology may augment this effect. Areas with high relief and soft lithology that is more prone to erosion

can increase the sediment loads of rivers (Ludwig and Probst, 1996). This in part explains the nonlinear relationship shown between discharge and sediment flux by this study. For example, Chinese rivers such as Mekong, Yellow and Yangtze that originate in the high relief Himalayan areas and flow through highly erosive loess plateau, have proportionately larger increases in sediment flux than discharge. However, the climate warming driven changes in vegetation patterns can also have effects on sediment loads due to the protection of soils against mechanical erosion (Ludwig and Probst, 1996), which is not considered in this analysis.

The aim of this study is to isolate the signal of climate on river discharge and sediment flux, hence the simulations are conducted under 'Pristine' conditions (see methodology). However, it is important to understand that human interventions and land use changes may have considerable effects on these predicted changes. Thus, the absolute values for discharge and sediment loads or directions and magnitudes of projected changes discussed in this study may considerably change depending on human activities and may not necessarily be realized in the future. The main idea behind this is to understand the changes that anthropogenic GHG emissions and associated global-warming induced temperatures and precipitation can bring about in global rivers and help informed decision making related to the management of large global rivers and formulate intelligent adaptation strategies for climate change impacts.

CHAPTER 5

CONCLUSION

In order to isolate the signal of projected future climate change on global riverine water discharge and suspended sediment fluxes in the 21st century, a numerical model (WBMsed) was forced with precipitation and temperature projections from five GCMs each driven by four RCPs. The results, based on an ensemble of model outputs, revealed that global river discharge and sediment fluxes will have considerable impacts in the 21st century due to climate change. These changes considerably vary through space and time and with different levels of GHG concentrations in the atmosphere. The forcing data used in the study shows that global land surface temperature increases toward the end of the century in all RCPs, and increases are larger with increasing warming scenarios. Global precipitation distribution varies between RCPs, leading to an overall increase in the mean global precipitation toward the end of the century in all scenarios.

River discharges are predicted to considerably increase in the Arctic, some regions in central Africa, south and east Asia, western parts of South America and northern Europe with increasing GHG-induced warming. In North America, most of the significant increasing trends are predicted for low and high warming scenarios. Significant decreases in river discharges can be expected over most of Europe, some regions in central Asia, southern regions of North America, central America, southern regions of Australia, and southern regions of South America under moderate and high RCP scenarios. In addition, some parts in central Africa, some of north

America, central regions of south America, and most of Australia will experience decreases in river discharge. Changes in sediment flux closely follow these patterns predicted for discharge. However, the relationship between discharge and sediment flux is nonlinear.

Despite regional differences, at a global scale, both mean global river discharge and sediment flux show a net increase in the 21st century under all RCP scenarios. The increase is generally larger with increasing RCP. At the end of this century, climate change under RCP 2.6 is projected to cause approximately 1% increase in global river discharge and 5% increase in global suspended sediment flux. Under RCP 4.5 emission scenario, climate change will lead to a 5.6% increase in river discharge and 7% increase in sediment flux at a global scale. Approximately 5% and 9% increases are projected under RCP 6.0 in global river discharge and sediment flux respectively. Climate changes projected under RCP 8.5, the highest GHG concentration scenario, will lead to the largest increases in river discharge and sediment flux (7.3% and 14.7% respectively) at the end of the 21st century. The rate of change in total global river discharge to the oceans in the 21st century due to climate change is projected to be +0.12% per decade under RCP 2.6, +0.5% per decade under RCP 4.5, +0.53% per decade under RCP 6.0 and +0.8% per decade under RCP 8.5. The rate of change in the 21st century total global sediment delivery to the oceans due to climate change alone is projected to be +0.7% per decade under RCP 2.6, +1% per decade under RCP 4.5, +1.3% per decade under RCP 6.0 and +1.8% per decade under RCP 8.5.

It is also evident that with increased warming scenarios, more extreme changes (increasing or decreasing) can be expected in both discharge and sediment flux, as well as in precipitation. Also, as warming increases the number of rivers with statistically significant trends (Mann-Kendall trend test, $p<0.05$) in either direction increases. In addition to the magnitudes,

temporal variability evaluated by CV shows that inter-annual variability in both river discharge and sediment flux also increases with increased GHG-induced warming. The patterns in inter-annual variability in discharge coincide with that of sediment flux, however the magnitude of the variability differ between the two variables. Based on the results it can be concluded that while global warming induced spatial and temporal variation in precipitation mainly drives discharge patterns and thus sediment dynamics under a changing climate, other factors such as relief and lithology may amplify this effect.

The analysis shows a considerable spread in the individual GCM responses, due to the different structures and parameters used in GCMs that resulted in different precipitation distribution patterns along with land surface warming. Considerable differences between individual GCM predictions and contrasting trends are reported widely in literature. This justifies the use of the multi-model ensemble in these kinds of studies. However, averaging the results of multiple GCM projections, may introduce some bias to the study. This method smoothens extremes projected by individual GCMs, and also in some instances one or two GCMs dominate the direction of change due to their high magnitude of discharge and sediment fluxes predicted. In addition to the uncertainties arise from the use of GCMs and their ensemble projections, other sources of uncertainties include the range of changes in climate conditions that can be captured by ISI-MIP climate models, future GHG concentration trajectories, and bias introduced by the WBMsed model accuracy.

It is also important to understand that these absolute values for discharge and sediment loads or directions and magnitudes of projected changes in response to climate change may considerably alter depending on human activities and future land use changes, and therefore may not necessarily be realized in the future. The findings of this study are useful to isolate the

changes that anthropogenic GHG emissions and associated global-warming induced temperatures and precipitation can bring about in large global rivers. This will help informed decision making related to the management of large global rivers and intelligent adaptation strategies for climate change impacts.

REFERENCES

Aerts, J.C.J.H., Renssen, H., Ward, P.J., De Moel, H., Odada, E., Bouwer, L.M. and Goosse, H., 2006. Sensitivity of global river discharges under Holocene and future climate conditions. *Geophysical Research Letters*, *33*(19).

Ahmed, A.A. and Ismail, U.H.A.E., 2008. Sediment in the Nile River system. *Consultancy Study requested by UNESCO*.

Alcamo, J., Flörke, M. and Märker, M., 2007. Future long-term changes in global water resources driven by socio-economic and climatic changes. *Hydrological Sciences Journal*, *52*(2), pp.247-275.

Arnell, N.W., 2003. Effects of IPCC SRES* emissions scenarios on river runoff: a global perspective. *Hydrology and Earth System Sciences Discussions*, *7*(5), pp.619-641.

Bates, B.C., Kundzewicz, Z.W., Wu, S., Palutikof, J.P. (Eds.), 2008. Climate Change and Water. Technical Paper of the Intergovernmental Panel on Climate Change, IPCC Secretariat, Geneva.

Bjørnæs, C., 2013. A guide to Representative Concentration Pathways. *CICERO. Center for International Climate and Environmental Research*.

Cai, X., Wang, D., Zhu, T. and Ringler, C., 2009. Assessing the regional variability of GCM simulations. *Geophysical Research Letters*, *36*(2).

Cohen, S., Kettner, A.J. and Syvitski, J.P., 2014. Global suspended sediment and water discharge dynamics between 1960 and 2010: Continental trends and intra-basin sensitivity. *global and planetary change*, *115*, pp.44-58.

Cohen, S., Kettner, A.J., Syvitski, J.P. and Fekete, B.M., 2013. WBMsed, a distributed global-scale riverine sediment flux model: Model description and validation. *Computers & geosciences*, *53*, pp.80-93.

Coulthard, T.J., Ramirez, J., Fowler, H.J. and Glenis, V., 2012. Using the UKCP09 probabilistic scenarios to model the amplified impact of climate change on drainage basin sediment yield. *Hydrology and Earth System Sciences*, *16*(11), pp.4401.

Covey, C., AchutaRao, K.M., Cubasch, U., Jones, P., Lambert, S.J., Mann, M.E., Phillips, T.J. and Taylor, K.E., 2003. An overview of results from the Coupled Model Intercomparison Project. *Global and Planetary Change*, *37*(1-2), pp.103-133.

Dai, A., Qian, T., Trenberth, K.E. and Milliman, J.D., 2009. Changes in continental freshwater discharge from 1948 to 2004. *Journal of climate*, *22*(10), pp.2773-2792.

Darby, S.E., Dunn, F.E., Nicholls, R.J., Rahman, M. and Riddy, L., 2015. A first look at the influence of anthropogenic climate change on the future delivery of fluvial sediment to the Ganges–Brahmaputra–Meghna delta. *Environmental Science: Processes & Impacts*, *17*(9), pp.1587-1600.

Döll, P. and Zhang, J., 2010. Impact of climate change on freshwater ecosystems: a global-scale analysis of ecologically relevant river flow alterations. *Hydrology and Earth System Sciences*, *14*(5), pp.783-799.

Flato, G., J. Marotzke, B. Abiodun, P. Braconnot, S.C. Chou, W. Collins, P. Cox, F. Driouech, S. Emori, V. Eyring, C. Forest, P. Gleckler, E. Guilyardi, C. Jakob, V. Kattsov, C. Reason and M. Rummukainen, 2013: Evaluation of Climate Models. In: *Climate Change 2013: The Physical Science Basis. Contribution of Working Group I to the Fifth Assessment Report of the Intergovernmental Panel on Climate Change* [Stocker, T.F., D. Qin, G.-K. Plattner, M. Tignor, S.K. Allen, J. Boschung, A. Nauels, Y. Xia, V. Bex and P.M. Midgley (eds.)]. Cambridge University Press, Cambridge, United Kingdom and New York, NY, USA.

Frieler, K., Lange, S., Piontek, F., Reyer, C.P., Schewe, J., Warszawski, L., Zhao, F., Chini, L., Denvil, S., Emanuel, K. and Geiger, T., 2017. Assessing the impacts of 1.5 C global warming–simulation protocol of the Inter-Sectoral Impact Model Intercomparison Project (ISIMIP2b). *Geoscientific Model Development*.

Fryirs, K., 2013. (Dis) Connectivity in catchment sediment cascades: a fresh look at the sediment delivery problem. *Earth Surface Processes and Landforms*, *38*(1), pp.30-46.

Gain, A.K., Immerzeel, W.W., Sperna Weiland, F.C. and Bierkens, M.F.P., 2011. Impact of climate change on the stream flow of the lower Brahmaputra: trends in high and low flows based on discharge-weighted ensemble modelling. *Hydrology and Earth System Sciences*, *15*(5), pp.1537-1545.

Haarsma, R.J., Selten, F.M., Weber, S.L. and Kliphuis, M., 2005. Sahel rainfall variability and response to greenhouse warming. *Geophysical Research Letters*, *32*(17).

Haddeland, I., Clark, D.B., Franssen, W., Ludwig, F., Voß, F., Arnell, N.W., Bertrand, N., Best, M., Folwell, S., Gerten, D. and Gomes, S., 2011. Multimodel estimate of the global terrestrial water balance: setup and first results. *Journal of Hydrometeorology*, *12*(5), pp.869-884.

Haddeland, I., Heinke, J., Biemans, H., Eisner, S., Flörke, M., Hanasaki, N., Konzmann, M., Ludwig, F., Masaki, Y., Schewe, J. and Stacke, T., 2014. Global water resources affected by human interventions and climate change. Proceedings of the National Academy of Sciences,111(9), pp.3251-3256.

Hagemann, S., Chen, C., Clark, D.B., Folwell, S., Gosling, S.N., Haddeland, I., Hanasaki, N., Heinke, J., Ludwig, F., Voss, F. and Wiltshire, A.J., 2013. Climate change impact on available water resources obtained using multiple global climate and hydrology models. *Earth System Dynamics*, *4*(1), pp.129-144.

Hattermann, F.F., Vetter, T., Breuer, L., Su, B., Daggupati, P., Donnelly, C., Fekete, B., Flörke, F., Gosling, S.N., Hoffmann, P. and Liersch, S., 2018. Sources of uncertainty in hydrological climate impact assessment: a cross-scale study. *Environmental Research Letters*, *13*(1), p.015006.

Hempel, S., Frieler, K., Warszawski, L., Schewe, J. and Piontek, F., 2013. A trend-preserving bias correction–the ISI-MIP approach. *Earth System Dynamics*, *4*(2), pp.219-236.

Hirabayashi, Y., Kanae, S., Emori, S., Oki, T. and Kimoto, M., 2008. Global projections of changing risks of floods and droughts in a changing climate. *Hydrological Sciences Journal*, *53*(4), pp.754-772.

IPCC SRES, N.N. and Swart, R., 2000. Special report on emissions scenarios: a special report of working group III of the Intergovernmental Panel on Climate Change.

IPCC, 2014: Climate Change 2014: Synthesis Report. Contribution of Working Groups I, II and III to the Fifth Assessment Report of the Intergovernmental Panel on Climate Change [Core Writing Team, R.K. Pachauri and L.A. Meyer (eds.)]. IPCC, Geneva, Switzerland, pp. 151.

ISIMIP, 2019. Inter-Sectoral Impact Model Intercomparison Project (accessed 03/29/2018) <https://www.isimip.org/gettingstarted/details/10/>

Julien, P.Y., 2010. *Erosion and sedimentation*. Cambridge University Press.

Kendall, M.G., 1975. Rank Correlation Methods, Griffin, London, UK.

Knutti, R. and Sedláček, J., 2013. Robustness and uncertainties in the new CMIP5 climate model projections. *Nature Climate Change*, *3*(4), p.369.

Krakauer, N.Y. and Fekete, B.M., 2014. Are climate model simulations useful for forecasting precipitation trends? Hindcast and synthetic-data experiments. *Environmental Research Letters*, *9*(2), p.024009.

Lange, S., 2019. Trend-preserving bias adjustment and statistical downscaling with ISIMIP3BASD (v1. 0). *Journal of Geoscientific Model Development Discussion* (In review).

López, J.C.R. and Torregroza, A.C., 2017. Suspended sediment load in northwestern South America (Colombia): A new view on variability and fluxes into the Caribbean Sea. *Journal of South American Earth Sciences*, *80*, pp.340-352.

Lu, X.X., Ran, L.S., Liu, S., Jiang, T., Zhang, S.R. and Wang, J.J., 2013. Sediment loads response to climate change: A preliminary study of eight large Chinese rivers. *International Journal of Sediment Research*, *28*(1), pp.1-14.

Ludwig, W. and Probst, J.L., 1996. A global modelling of the climatic, morphological, and lithological control of river sediment discharges to the oceans. *IAHS Publications-Series of Proceedings and Reports-Intern Assoc Hydrological Sciences*, *236*, pp.21-22.

Mann, H. B., 1945. Nonparametric tests against trend, Econometrica, 13, pp. 245-259.

Masood, M., Yeh, P.F., Hanasaki, N. and Takeuchi, K., 2015. Model study of the impacts of future climate change on the hydrology of Ganges–Brahmaputra–Meghna basin. *Hydrology and Earth System Sciences*, *19*(2), pp.747-770.

Materia, S., Dirmeyer, P.A., Guo, Z., Alessandri, A. and Navarra, A., 2010. The sensitivity of simulated river discharge to land surface representation and meteorological forcings. *Journal of Hydrometeorology*, *11*(2), pp.334-351.

McSweeney, C.F. and Jones, R.G., 2016. How representative is the spread of climate projections from the 5 CMIP5 GCMs used in ISI-MIP?. *Climate Services*, *1*, pp.24-29.

Milliman, J.D. and Meade, R.H., 1983. World-wide delivery of river sediment to the oceans. *The Journal of Geology*, *91*(1), pp.1-21.

Milliman, J.D. and Syvitski, J.P., 1992. Geomorphic/tectonic control of sediment discharge to the ocean: the importance of small mountainous rivers. *The Journal of Geology*, *100*(5), pp.525-544.

Milliman, J.D., Steele, J.H., Thorpe, S.A. and Turekian, K.K., 2001. River inputs.

Milly, P.C., Dunne, K.A. and Vecchia, A.V., 2005. Global pattern of trends in streamflow and water availability in a changing climate. *Nature*, *438*(7066), p.347.

Morehead, M.D., Syvitski, J.P., Hutton, E.W. and Peckham, S.D., 2003. Modeling the temporal variability in the flux of sediment from ungauged river basins. *Global and Planetary change*, *39*(1-2), pp.95-110.

Mouyen, M., Longuevergne, L., Steer, P., Crave, A., Lemoine, J.M., Save, H. and Robin, C., 2018. Assessing modern river sediment discharge to the ocean using satellite gravimetry. *Nature communications*, *9*(1), p.3384.

Mukundan, R., Pradhanang, S.M., Schneiderman, E.M., Pierson, D.C., Anandhi, A., Zion, M.S., Matonse, A.H., Lounsbury, D.G. and Steenhuis, T.S., 2013. Suspended sediment source areas and future climate impact on soil erosion and sediment yield in a New York City water supply watershed, USA. *Geomorphology*, *183*, pp.110-119.

Mulder, T. and Syvitski, J.P.M., 1996. Climatic and morphologic relationships of rivers: implications of sea-level fluctuations on river loads. *The Journal of Geology*, *104*(5), pp.509-523.

Nakaegawa, T., Kitoh, A. and Hosaka, M., 2013. Discharge of major global rivers in the late 21st century climate projected with the high horizontal resolution MRI - AGCMs. *Hydrological Processes*, *27*(23), pp.3301-3318.

Nijssen, B., O'donnell, G.M., Hamlet, A.F. and Lettenmaier, D.P., 2001. Hydrologic sensitivity of global rivers to climate change. *Climatic change*, *50*(1-2), pp.143-175.

Nohara, D., Kitoh, A., Hosaka, M. and Oki, T., 2006. Impact of climate change on river discharge projected by multimodel ensemble. *Journal of Hydrometeorology*, *7*(5), pp.1076-1089.

Oki, T. and Kanae, S., 2006. Global hydrological cycles and world water resources. Science, *313*(5790), pp.1068-1072.

Pelletier, J.D., 2012. A spatially distributed model for the long-term suspended sediment discharge and delivery ratio of drainage basins. *Journal of Geophysical Research: Earth Surface*, *117*(F2).

Pendergrass, A.G., Knutti, R., Lehner, F., Deser, C. and Sanderson, B.M., 2017. Precipitation variability increases in a warmer climate. *Scientific reports*, *7*(1), pp.17966.

Rodríguez-Blanco, M.L., Arias, R., Taboada-Castro, M.M., Nunes, J.P., Keizer, J.J. and Taboada-Castro, M.T., 2016. Potential Impact of Climate Change on Suspended Sediment Yield in NW Spain: A Case Study on the Corbeira Catchment. *Water*, *8*(10), pp.444.

Schewe, J., Heinke, J., Gerten, D., Haddeland, I., Arnell, N.W., Clark, D.B., Dankers, R., Eisner, S., Fekete, B.M., Colón-González, F.J. and Gosling, S.N., 2014. Multimodel assessment of water scarcity under climate change. *Proceedings of the National Academy of Sciences*, *111*(9), pp.3245-3250.

Shrestha, B., Cochrane, T.A., Caruso, B.S., Arias, M.E. and Piman, T., 2016. Uncertainty in flow and sediment projections due to future climate scenarios for the 3S Rivers in the Mekong Basin. *Journal of Hydrology*, *540*, pp.1088-1104.

Sperna Weiland, F.C., Van Beek, L.P.H., Kwadijk, J.C.J. and Bierkens, M.F.P., 2012. Global patterns of change in discharge regimes for 2100. *Hydrology and Earth System Sciences*, *16*, pp.1047-1062.

Sylla, M.B., Nikiema, P.M., Gibba, P., Kebe, I. and Klutse, N.A.B., 2016. Climate change over West Africa: Recent trends and future projections. In *Adaptation to climate change and variability in rural West Africa* (pp. 25-40). Springer, Cham.

Syvitski, J.P., 2002. Sediment discharge variability in Arctic rivers: implications for a warmer future. *Polar Research*, *21*(2), pp.323-330.

Syvitski, J.P., 2003a, September. The influence of climate on the flux of sediment to the coastal ocean. In *OCEANS 2003. Proceedings* (Vol. 2, pp. 981-985). IEEE.

Syvitski, J.P., 2003b. Supply and flux of sediment along hydrological pathways: research for the 21st century. *Global and Planetary Change*, *39*(1), pp.1-11.

Syvitski, J.P., Cohen, S., Kettner, A.J. and Brakenridge, G.R., 2014. How important and different are tropical rivers?—An overview. *Geomorphology*, *227*, pp.5-17.

Syvitski, J.P., Milliman, J.D., 2007. Geology, geography, and humans battle for dominance over the delivery of fluvial sediment to the coastal ocean. J. Geol.115 (1), pp.1–19.

Syvitski, J.P., Peckham, S.D., Hilberman, R. and Mulder, T., 2003. Predicting the terrestrial flux of sediment to the global ocean: a planetary perspective. *Sedimentary Geology*, *162*(1), pp.5-24.

Syvitski, J.P., Vörösmarty, C.J., Kettner, A.J. and Green, P., 2005. Impact of humans on the flux of terrestrial sediment to the global coastal ocean. *science*, *308*(5720), pp.376-380.

Taylor, P.G., Wieder, W.R., Weintraub, S., Cohen, S., Cleveland, C.C. and Townsend, A.R., 2015. Organic forms dominate hydrologic nitrogen export from a lowland tropical watershed. Ecology, 96(5), pp.1229-1241.

Teng, J., Vaze, J., Chiew, F.H., Wang, B. and Perraud, J.M., 2012. Estimating the relative uncertainties sourced from GCMs and hydrological models in modeling climate change impact on runoff. *Journal of Hydrometeorology*, *13*(1), pp.122-139.

Trenberth, K.E., 2011. Changes in precipitation with climate change. *Climate Research*, *47*(1-2), pp.123-138.

U.S. Geological Survey, 2018. National Water Information System data (Water Data for the Nation). (accessed 05/06/2018) <http://waterdata.usgs.gov/nwis/>.

Uhe, P., Mitchell, D., Bates, P., Sampson, C., Smith, A. and ISLAM, A.S., 2019. Enhanced flood risk with 1.5° C global warming in the Ganges-Brahmaputra-Meghna basin. *Environmental Research Letters*.

van Vliet, M.T., Franssen, W.H., Yearsley, J.R., Ludwig, F., Haddeland, I., Lettenmaier, D.P. and Kabat, P., 2013. Global river discharge and water temperature under climate change. *Global Environmental Change*, *23*(2), pp.450-464.

Van Vuuren, D.P., Edmonds, J., Kainuma, M., Riahi, K., Thomson, A., Hibbard, K., Hurtt, G.C., Kram, T., Krey, V., Lamarque, J.F. and Masui, T., 2011. The representative concentration pathways: an overview. *Climatic change*, *109*(1-2), p.5.

Vercruysse, K., Grabowski, R.C. and Rickson, R.J., 2017. Suspended sediment transport dynamics in rivers: multi-scale drivers of temporal variation. Earth-science reviews, 166, pp.38-52.

Vörösmarty, C. J., Green, P., Salisbury, J., and Lammers, R. B. 2000. Global water resources: Vulnerability from climate change and population growth, Science, 289, 284–288.

Vörösmarty, C.J., Meybeck, M., Fekete, B., Sharma, K., Green, P., Syvitski, J.P.M., 2003. Anthropogenic sediment retention: major global impact from registered river impoundments. Glob. Planet. Chang. 39 (1–2), pp.169–190.

Walling, D. E. and Fang, D., 2003. Recent trends in the suspended sediment loads of the world's rivers. Global Planet. Change, 39, pp.111–126.

Walling, D.E. and Webb, B.W., 1983. Dissolved Loads of Rivers: A Global Overview.

Walling, D.E. and Webb, B.W., 1996. Erosion and sediment yield: a global overview. *IAHS Publications-Series of Proceedings and Reports-Intern Assoc Hydrological Sciences*, *236*, pp.3-20.

Walling, D.E., 1997. The response of sediment yields to environmental change. *IAHS Publication*, *245*, pp.77-89.

Walling, D.E., 2009. *The impact of global change on erosion and sediment transport by rivers: current progress and future challenges*. UNESCO.

Wang, H., Saito, Y., Zhang, Y., Bi, N., Sun, X. and Yang, Z., 2011. Recent changes of sediment flux to the western Pacific Ocean from major rivers in East and Southeast Asia. *Earth-Science Reviews*, *108*(1-2), pp.80-100.

Ward, P.J., van Balen, R.T., Verstraeten, G., Renssen, H. and Vandenberghe, J., 2009. The impact of land use and climate change on late Holocene and future suspended sediment yield of the Meuse catchment. *Geomorphology*, *103*(3), pp.389-400.

Warszawski, L., Frieler, K., Huber, V., Piontek, F., Serdeczny, O. and Schewe, J., 2014. The inter-sectoral impact model intercomparison project (ISI–MIP): project framework. *Proceedings of the National Academy of Sciences*, *111*(9), pp.3228-3232.

Weedon G P, Gomes S, Viterbo P, Shuttleworth W J, Blyth E, Osterle H, Adam J C, Bellouin N, Boucher O and Best M. 2011. Creation of the watch forcing data and its use to assess global and regional reference crop evaporation over land during the twentieth century *J. Hydrometeorol.* **12** 823–48.

Wilson, L., 1973. Variations in mean annual sediment yield as a function of mean annual precipitation. *American Journal of Science*, *273*(4), pp.335-349.

Yang, D., Kanae, S., Oki, T., Koike, T., Musiake, K., 2003. Global potential soil erosion with reference to land use and climate changes. Hydrological Processes 17, 2913–2928.

Yang, S.L., Xu, K.H., Milliman, J.D., Yang, H.F. and Wu, C.S., 2015. Decline of Yangtze River water and sediment discharge: Impact from natural and anthropogenic changes. *Scientific reports*, *5*, p.12581.

Zhu, Q., Jiang, H., Peng, C., Liu, J., Fang, X., Wei, X., Liu, S. and Zhou, G., 2012. Effects of future climate change, CO2 enrichment, and vegetation structure variation on hydrological processes in China. *Global and planetary change*, *80*, pp.123-135.

Zhu, Y.M., Lu, X.X. and Zhou, Y., 2008. Sediment flux sensitivity to climate change: A case study in the Longchuanjiang catchment of the upper Yangtze River, China. *Global and Planetary Change*, *60*(3-4), pp.429-442.

APPENDIX

Detailed Analysis of selected major river outlets

The eight major river outlets selected for further investigation of climate change induced future trends in discharge and sediment flux represent different continents, latitudinal regions and various climatic zones. These river outlets are major contributors of discharge and sediment flux to the global oceans from their continents, and most of them have highly populated and vulnerable river deltas. Thus, it is vital to understand the changes that can happen in these rivers in response to future climate projections. In fact, it is important to understand that these changes are predicted based on "pristine" simulations under future climate change trajectories, thus in the real world they may have highly regulated water and sediment discharges to the global ocean due to human activities and land use changes.

Amazon

The Amazon River located in the tropical region is rated number one in the world in terms of drainage area and water discharge to the ocean (Milliman, and Meade, 1983) and is among the largest contributors of sediment load to the ocean (Milliman et al., 2001; Mouyen et al., 2018). Different RCP scenarios resulted in difference responses of discharge and sediment supply to the ocean at the Amazon River outlet. Basin-averaged temperature increases with increasing warming scenario (Figure 18). Under RCP 2.6, a significant decrease in (Mann Kendall, $p<0.05$) in discharge and a slight decrease in sediment flux was predicted in response to

a negative trend in precipitation. Under RCP 4.5, both discharge and sediment flux show an increase toward the end of the century, increase in sediment flux being significant ($p<0.05$). This is mainly due to the increasing trend in precipitation.

Although there is a decreasing trend in precipitation under RCP 6.0, discharge or sediment flux does not show any significant trend during the 21st century. The RCP 8.5 scenario show a significant increase in both discharge and sediment flux ($p<0.05$) as a result of the increase in precipitation. Although these projections cannot be directly compared with other studies as they have used a previous set of climate change scenarios introduced prior to the most recent report of the IPCC, Nakaegawa et al. (2013) found a projected decrease in discharge over the southern half of the Amazon river under moderate warming scenario, and Nohara et al. (2006) projected a slight increase under moderate warming scenario.

Figure 18: Time series of mean annual river discharge (a) mean annual sediment flux in the river outlet (b) mean annual precipitation total for the basin (c) and basin-averaged temperature (d) for each RCP scenario in the Amazon river.

Danube

The Danube River has the largest drainage area and river discharge in Europe along with a large proportion of the continent's sediment flux (Milliman and Meade, 1983). This mid-latitudinal river is predicted to face a decrease in discharge and sediment loads with increasing climate warming (Aerts et al., 2006; Nohara et al., 2006; Sperna Weiland et al., 2012). However, under low warming scenario, discharge and sediment supply from the Danube river outlet will increase toward the end of the 21st century due to increasing precipitation. The increase in sediment supply under this scenario is significant (Mann-Kendall, $p<0.05$). Under all the moderate and high warming scenarios, this river is projected to experience a significant decrease in discharge and sediment flux to the ocean. This is in agreement with the predicted reduction in precipitation over the continental Europe (Rodríguez-Blanco et al., 2016).

Figure 19: Time series of mean annual river discharge (a) mean annual sediment flux in the river outlet (b) mean annual precipitation total for the basin (c) and basin-averaged temperature (d) for each RCP scenario in the Danube river.

Ganges-Brahmaputhra

Ganges-Brahmaputhra carries the largest river sediment load in the world (Milliman and Meade, 1983), draining the Himalaya-Tibetan plateau region. This Asian, monsoon-driven river shows high sensitivity to future climate change. Under all climate warming scenarios this river's discharge and sediment supply to the Indian ocean increases significantly in the 21st century. This is consistent with other studies such as Darby et al. (2015) that found an increase in both discharge and sediment flux under moderate climate scenarios and Gain et al., (2011), Masood et al. (2015) and Uhe et al. (2019), who found increases in peak discharge and flood hazard in the basin under moderate and high climate warming.

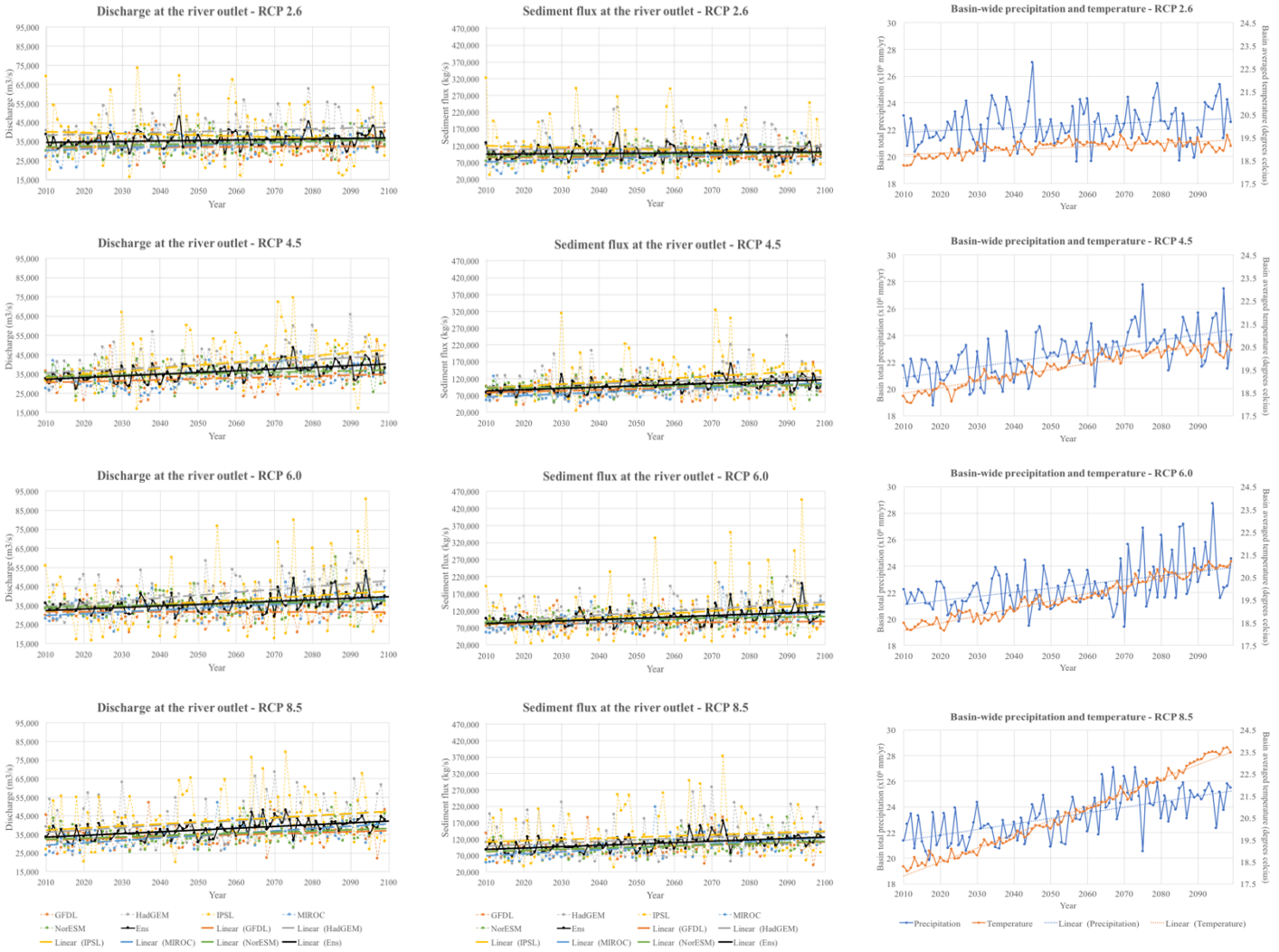

Figure 20: Time series of mean annual river discharge (a) mean annual sediment flux in the river outlet (b) mean annual precipitation total for the basin (c) and basin-averaged temperature (d) for each RCP scenario in the Ganges-Brahmaputhra rivers.

Lena

Lena river located in the high latitudes of the Arctic where large increases in temperature, precipitation, and discharge are projected by a number of studies (Milly et al., 2005; Nakaegawa et al., 2013; Nohara et al., 2006; Sperna Weiland et al., 2012). This study also shows that significant increases in discharge can be expected in Lena river outlet under all climate change scenarios, while significant increases in sediment flux can be expected for RCP 4.5, 6.0 and 8.5 scenarios. The reason for this is the projected increase in temperature and precipitation over this river basin (Aerts et al., 2006; Bates et al., 2008).

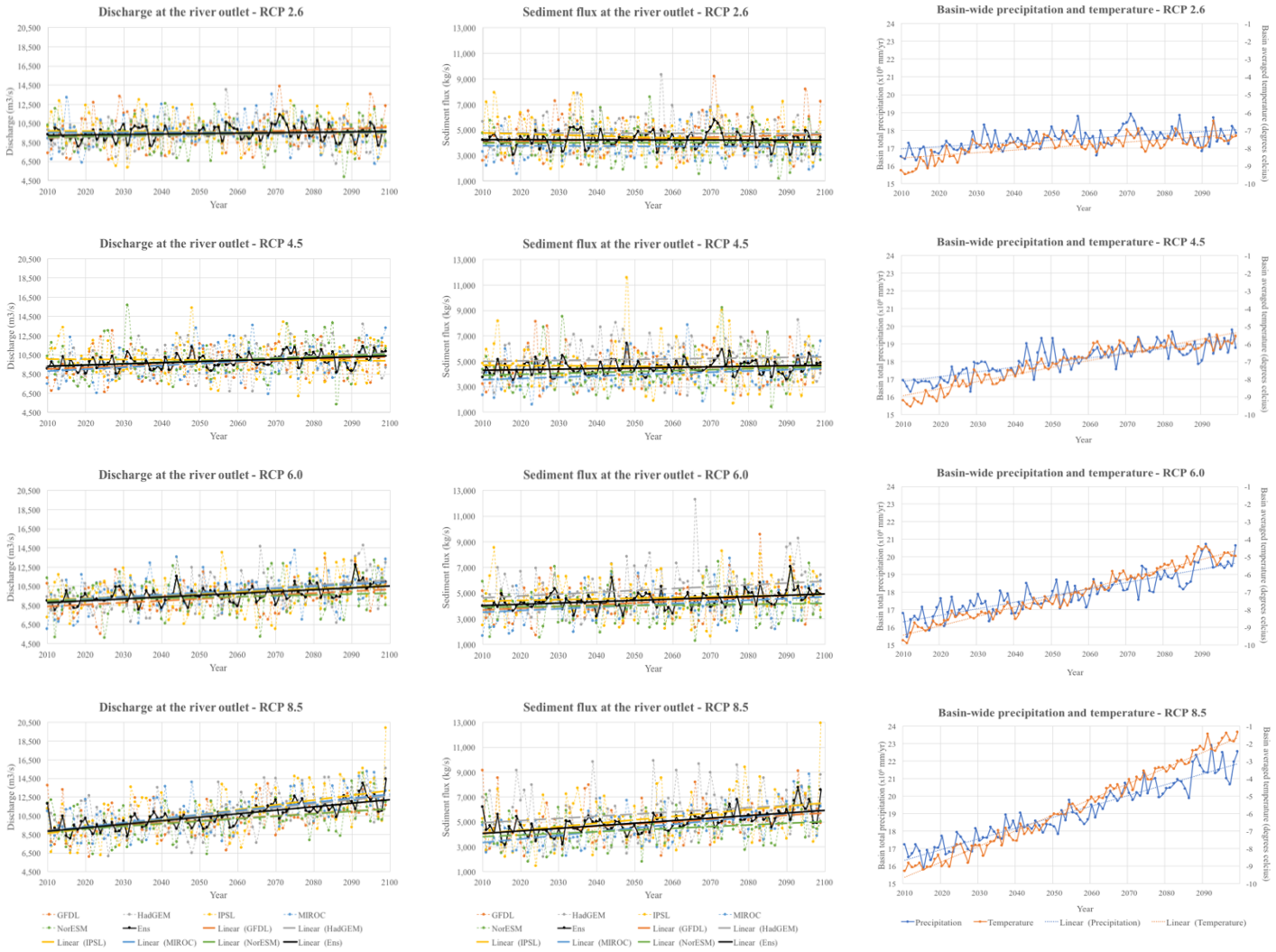

Figure 21: Time series of mean annual river discharge (a) mean annual sediment flux in the river outlet (b) mean annual precipitation total for the basin (c) and basin-averaged temperature (d) for each RCP scenario in the Lena river.

Mississippi

Mississippi river in mid latitudinal region that drains much of the North America, carries large sediment loads to the Gulf of Mexico (Milliman, and Meade, 1983). Under RCP 2.6, a slight increase in discharge and a significant increase in sediment flux to the ocean can be seen in this river outlet, followed by an increase in precipitation. If RCP 4.5 scenario is realized, there will be no significant change in discharge and sediment flux in the 21st century. However, in agreement with other studies (e.g. Aerts et al., 2006; Hagemann et al., 2013; van Vliet et al., 2013) that showed discharge decreases under moderate to high warming scenarios, this study also predicts significant discharge reductions from the Mississippi river outlet under RCP 6.0 and 8.5. Sediment flux under these two scenarios also decrease, however, they are not significant.

Figure 22: Time series of mean annual river discharge (a) mean annual sediment flux in the river outlet (b) mean annual precipitation total for the basin (c) and basin-averaged temperature (d) for each RCP scenario in the Mississippi river.

Nile

Nile river basin with its majority situated in arid and semi-arid region in Africa (Ahmed and Ismail, 2008) shows sensitivity to moderate and high levels of climate change. Under RCP 6.0 and 8.5 scenarios significant increases in both river discharge and sediment flux can be seen in this river. The increase in discharge is also significant under RCP 4.5. Although discharge in RCP 2.6 and sediment flux in RCP 2.6 and 4.5 show increasing trends in the 21st century, they are not significant. This prediction is in agreement with other studies such as Nakaegawa et al. (2013), that shows significant increases in discharge with moderate warming. This is mainly due to the increase in precipitation predicted for central Africa where a large proportion of the river basin is located (Aerts et al., 2006; Nohara et al., 2006).

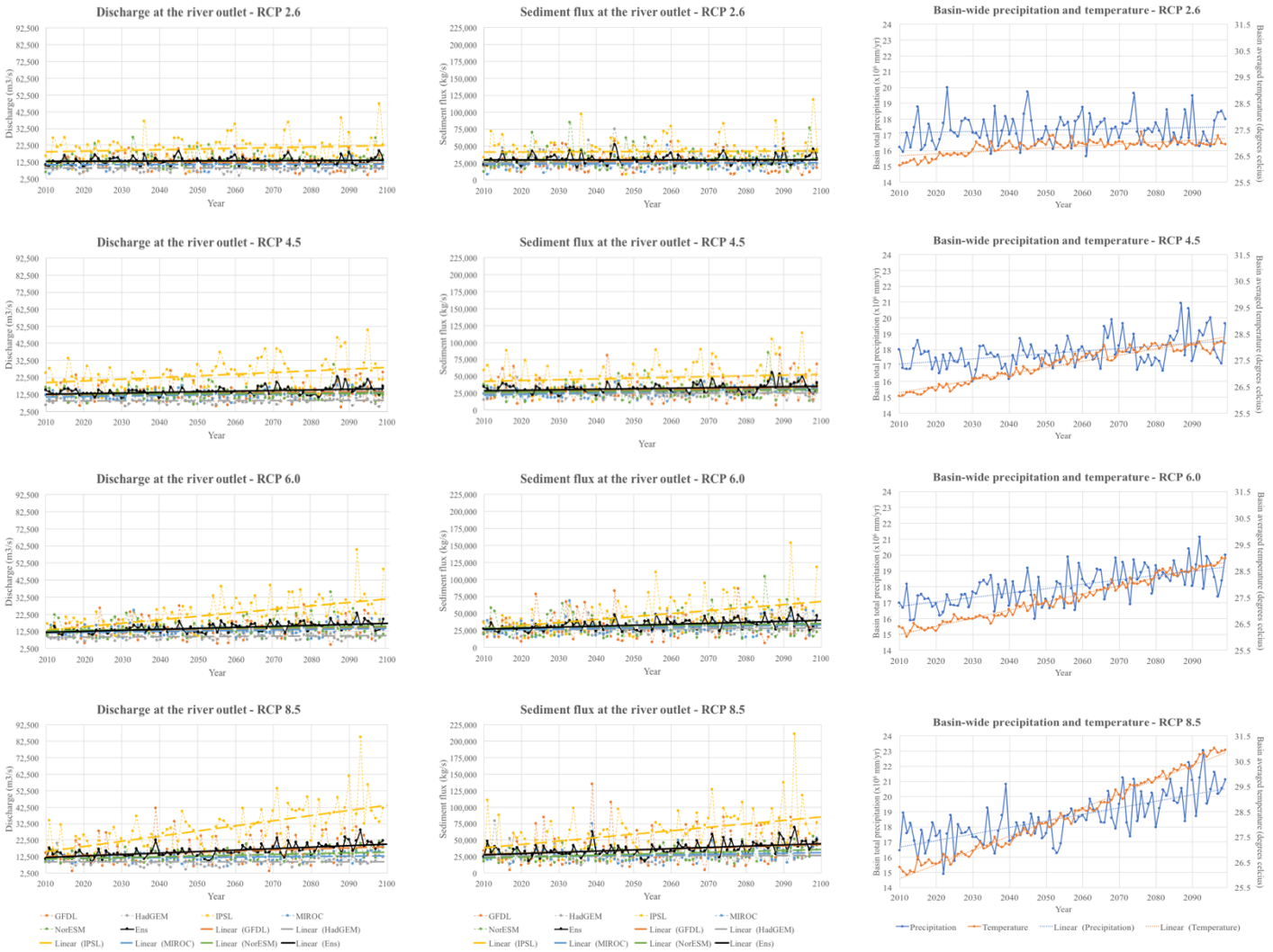

Figure 23: Time series of mean annual river discharge (a) mean annual sediment flux in the river outlet (b) mean annual precipitation total for the basin (c) and basin-averaged temperature (d) for each RCP scenario in the Nile river.

Parana

The second largest drainage system in the South American continent, Parana river's discharge or sediment loads, does not show much sensitivity to predicted future climate changes. Under all climate change scenarios decreases in precipitation are projected for this river basin, however, discharge and sediment flux to the Atlantic Ocean does not show significant changes in the 21st century under any of these scenarios.

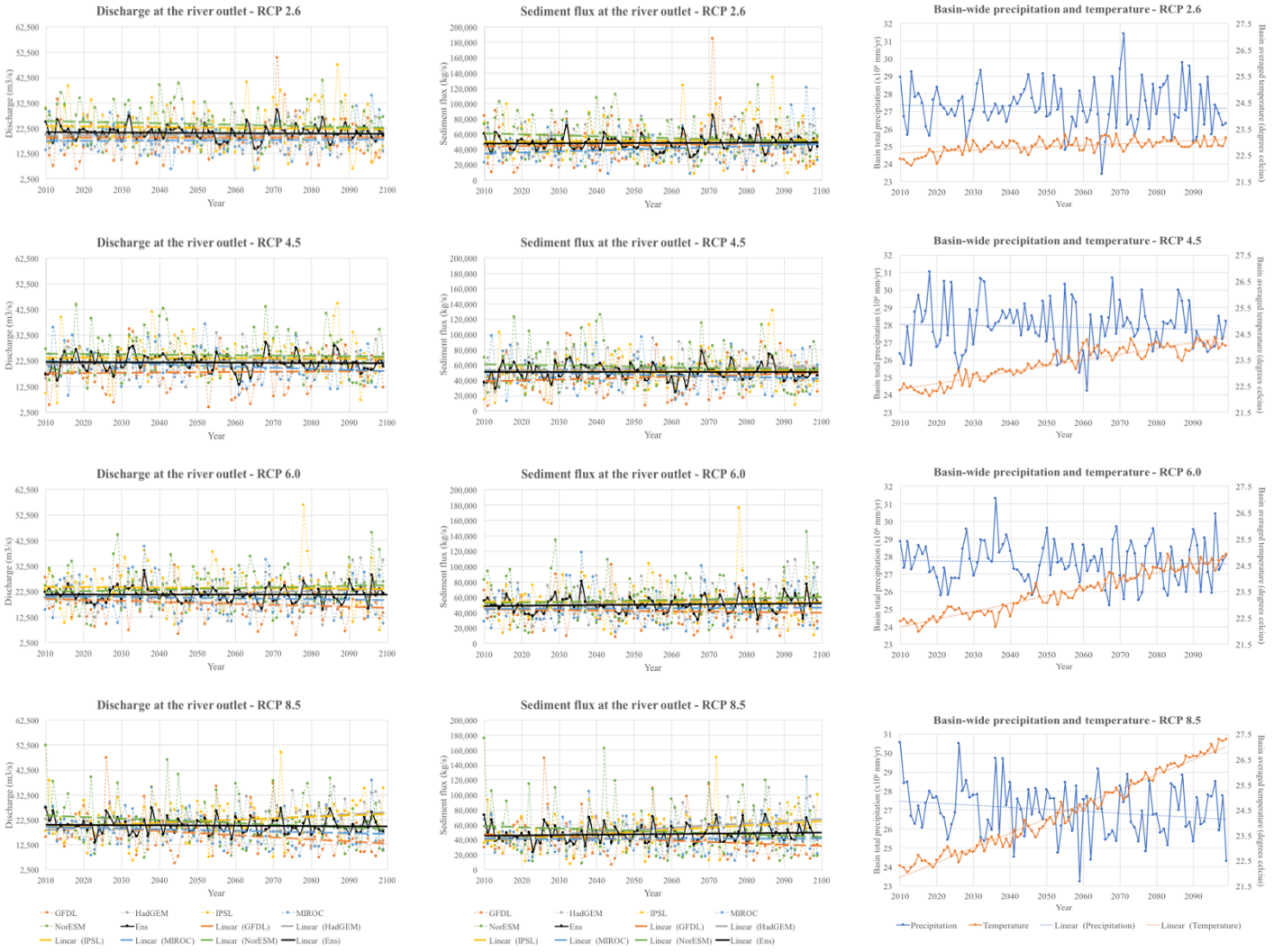

Figure 24: Time series of mean annual river discharge (a) mean annual sediment flux in the river outlet (b) mean annual precipitation total for the basin (c) and basin-averaged temperature (d) for each RCP scenario in the Parana river.

Yangtze

Yangtze river originates in the highlands of the Himalaya-Tibetan Plateau and is a large contributor of sediment to the Western Pacific Ocean (Wang et al., 2011). This study shows that Yangtze river discharge and sediment flux will have significant changes in response to future climate changes. Under all RCP scenarios (except for RCP 6.0) discharge can be expected to significantly increase, while under all climate change scenarios sediment flux to the ocean show significant increasing trends in the 21st century. This is in relation to the predicted increases in precipitation over the east Asia. Sperna Weiland et al. (2012) and Nohara et al. (2006) have also found increasing river discharge in Yangtze under moderate levels of climate change.

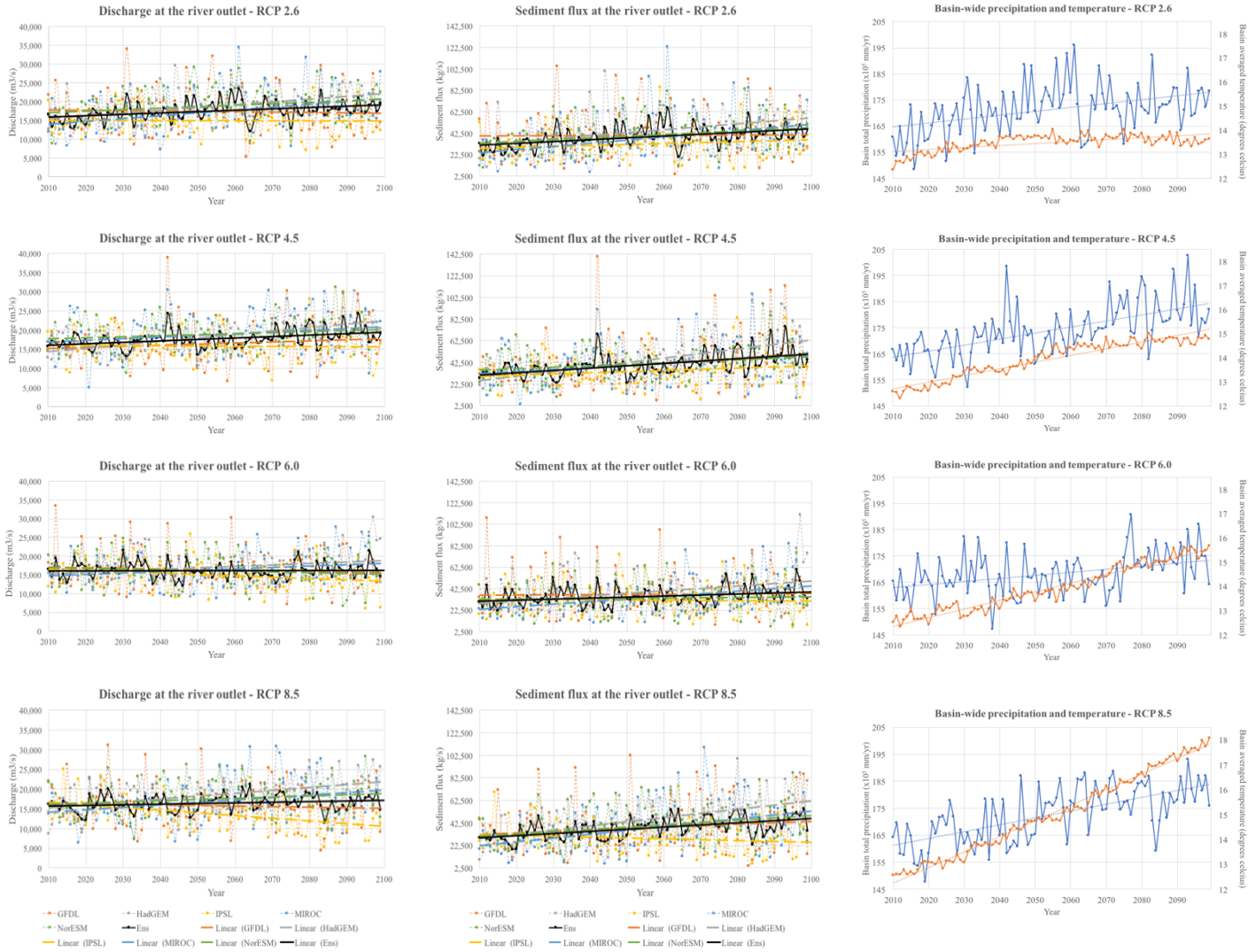

Figure 25: Time series of mean annual river discharge (a) mean annual sediment flux in the river outlet (b) mean annual precipitation total for the basin (c) and basin-averaged temperature (d) for each RCP scenario in the Yangtze river.